
Does Adversarial Transferability Indicate Knowledge Transferability?

Kaizhao Liang*

Department of Computer Science

University of Illinois at Urbana Champaign

Champaign, IL 61801

kl2@illinois.edu

Jacky Y. Zhang*

Department of Computer Science

University of Illinois at Urbana Champaign

Champaign, IL 61801

yiboz@illinois.edu

Oluwasanmi Koyejo

Department of Computer Science

University of Illinois at Urbana Champaign

Champaign, IL 61801

sanmi@illinois.edu

Bo Li

Department of Computer Science

University of Illinois at Urbana Champaign

Champaign, IL 61801

lbo@illinois.edu

Abstract

Despite the immense success that deep neural networks (DNNs) have achieved, *adversarial examples*, which are perturbed inputs that aim to mislead DNNs to make mistakes, have recently led to great concern. On the other hand, adversarial examples exhibit interesting phenomena, such as *adversarial transferability*. DNNs also exhibit knowledge transfer, which is critical to improving learning efficiency and learning in domains that lack high-quality training data. In this paper, we aim to turn the existence and pervasiveness of adversarial examples into an advantage. Given that adversarial transferability is easy to measure while it can be challenging to estimate the effectiveness of knowledge transfer, *does adversarial transferability indicate knowledge transferability?* We first theoretically analyze the relationship between adversarial transferability and knowledge transferability and outline easily checkable sufficient conditions that identify when adversarial transferability indicates knowledge transferability. In particular, we show that composition with an affine function is sufficient to reduce the difference between two models when adversarial transferability between them is high. We provide empirical evaluation for different transfer learning scenarios on diverse datasets, including CIFAR-10, STL-10, CelebA, and Taskonomy-data – showing a strong positive correlation between the adversarial transferability and knowledge transferability, thus illustrating that our theoretical insights are predictive of practice.

1 Introduction

Knowledge transferability, also known as learning transferability, has attracted extensive study in machine learning. Long before it was formally defined, the computer vision community has exploited it to perform important visual manipulations [30], such as style transfer and super-resolution, where pretrained VGG networks [63] are utilized to encode images into semantically meaningful features. After the release of ImageNet [56], pretrained ImageNet models (e.g., on TensorFlow Hub or PyTorch-Hub) has quickly become the default option for the transfer source, because of its broad coverage of visual concepts and compatibility with various visual tasks [26]. Numerous visual tasks, especially

*equal contribution

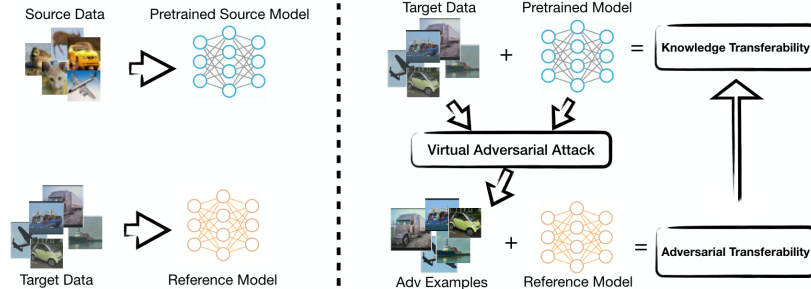


Figure 1: A simple illustration of the relationship between adversarial and knowledge transferability.

the ones whose annotations are expensive to obtain, rely heavily on having a good pretrained model. However, a recent study shows that the ImageNet models are not only unrobust against noise but also biased towards textures [14]. Simultaneously, as more and more datasets are published, more and more tasks are formulated. It is dauntingly difficult to brute-force evaluating all of them in search of the optimal pretrained model – since there is no effective measurement of knowledge transferability in practice. Therefore, now more than ever, we urgently need a method that can efficiently measure and identify promising candidates from the increasingly large pool of pretrained models.

Here is where the adversarial transferability comes to the rescue. It is discovered that neural networks are susceptible to adversarial examples, and more intriguingly, these adversarial examples can not only target the model they are generated from but also affect other models [16, 51]. This phenomenon is called adversarial transferability, which is extensively exploited to inspire black-box attacks[27, 38]. Many theoretical analyses have been conducted to establish the sufficient conditions of adversarial transferability [8, 44]. Despite their malicious potential, some observations indicate that an adversarial example can reveal the vital properties of neural networks [28]. It reflects hidden cues important for decision-making, that are otherwise imperceptible for the mortal eyes. Besides, it is usually easier to measure the adversarial transferability between two models by generating adversarial examples directly than fine-tuning. This inspires us to investigate the underlying relation between adversarial transferability and knowledge transferability. We aim to leverage the adversarial transferability as a surrogate to approximate the knowledge transfer behavior as shown in Figure 1. We believe this will lead to an efficient knowledge transfer mechanism.

To the best of our knowledge, this is the first work to show that adversarial transferability indicates knowledge transferability both theoretically and empirically². Our main contributions follow.

- We formally define two quantities, τ_1 and τ_2 , to *measure adversarial transferability from different aspects*, which for the first time enables in-depth understanding of adversarial transferability from a geometric point of view in the feature representation space.
- We derive an *upper bound for knowledge transferability with respect to adversarial transferability*. We rigorously depict their underlying relation and show that adversarial transferability can indicate knowledge transferability.
- We conduct thorough controlled experiments for diverse knowledge transfer scenarios (e.g. knowledge transfer among data distributions, attributes, and tasks) on benchmark datasets including STL-10, CIFAR-10, CelebA, and Taskonomy-data. Our empirical results show *strong positive correlation* between adversarial and knowledge transferability, which validates our theoretical conclusions.

Related work. *Knowledge transferability* has been widely applied in scenarios where the available data for certain domain or task is limited, and has achieved great success [73, 77, 75, 33, 45, 10]. Several studies have been conducted to understand the reasons and factors that affect knowledge transferability [80, 41, 76, 79, 62]. Empirical observations show that the correlation between learning tasks [1, 82], the similarity of model architectures, and data distribution are all correlated with different knowledge transfer effects. However, a more effective indicator of knowledge transferability is required to quantitatively understand its effectiveness or feasibility in a computational realistic way even before one conducts the expensive training and fine-tuning process.

Adversarial Transferability has been observed by several works [51, 16, 31]. Since the early work, a

²Code available at <https://github.com/AI-secure/Does-Adversarial-Transferability-Indicate-Knowledge-Transferability>

lot of studies have been conducted, aiming to further understand the phenomenon and design more transferable adversarial attacks. Regardless of the threat model, a lot of attack methods have been proposed to boost adversarial transferability [84, 8, 11, 78]. Naseer et al. [48] propose to produce adversarial examples that transfer cross-domain via a generative adversarial network. In addition to the efficacy, efficiency [27] and practicality [52] are also optimized. Beyond the above empirical studies, there is some work dedicated to analyzing this phenomenon, showing different conditions that may enhance adversarial transferability [2, 70, 44, 8]. Building upon these observations, it is clear that there exist certain connections between adversarial transferability and other knowledge transfer scenarios, and here we aim to provide the first theoretic justification to verify it and design systematic empirical studies to measure such correlation.

2 Adversarial Transferability vs. Knowledge Transferability

In this section, we establish connections between adversarial examples and knowledge transferability rigorously. We first formally state the problem studied in this section. Then, we move on to subsection 2.1 to introduce two metrics that encode information about adversarial attacks. Finally, we present our theoretical results about the relationship between adversarial and knowledge transferability in subsection 2.2.

Notation. We use blackboard bold to denote sets, e.g., \mathbb{R} . We use calligraphy to denote distributions, e.g., \mathcal{D} . The support of a distribution \mathcal{D} is denoted as $\text{supp}(\mathcal{D})$. We use bold lower case letters to denote vectors, e.g., $\mathbf{x} \in \mathbb{R}^n$. We use bold uppercase letter to denote a matrix, e.g., \mathbf{A} . We use \mathbf{A}^\dagger to denote the Moore–Penrose inverse of matrix \mathbf{A} . We use \circ to denote the composition of functions, i.e., $g \circ f(\mathbf{x}) = g(f(\mathbf{x}))$. We use $\|\cdot\|_2$ to denote Euclidean norm induced by standard inner product $\langle \cdot, \cdot \rangle$. Given a function f , we use $f(\mathbf{x})$ to denote its evaluated value at \mathbf{x} , and we use f to represent this function in function space. We use $\langle \cdot, \cdot \rangle_{\mathcal{D}}$ to denote inner product induced by distribution \mathcal{D} , i.e., $\langle f_1, f_2 \rangle_{\mathcal{D}} = \mathbb{E}_{\mathbf{x} \sim \mathcal{D}} \langle f_1(\mathbf{x}), f_2(\mathbf{x}) \rangle$. Accordingly, we use $\|\cdot\|_{\mathcal{D}}$ to denote a norm induced by inner product $\langle \cdot, \cdot \rangle_{\mathcal{D}}$, i.e., $\|f\|_{\mathcal{D}} = \sqrt{\langle f, f \rangle_{\mathcal{D}}}$. For a matrix function $F : \text{supp}(\mathcal{D}) \rightarrow \mathbb{R}^{d \times m}$, we define its $L^2(\mathcal{D})$ -norm in accordance with matrix 2-norm as $\|F\|_{\mathcal{D}, 2} = \sqrt{\mathbb{E}_{\mathbf{x} \sim \mathcal{D}} \|F(\mathbf{x})\|_2^2}$. We define projection operator $\text{proj}(\cdot, r)$ to project a matrix to a hyperball of spectral norm radius r , i.e.,

$$\text{proj}(\mathbf{A}, r) = \begin{cases} \mathbf{A}, & \text{if } \|\mathbf{A}\|_2 \leq r \\ r\mathbf{A}/\|\mathbf{A}\|_2 & \text{if } \|\mathbf{A}\|_2 > r \end{cases}.$$

Setting. Assume we are given a target problem defined by data distribution $\mathbf{x} \sim \mathcal{D}$, where $\mathbf{x} \in \mathbb{R}^n$, and $y : \mathbb{R}^n \rightarrow \mathbb{R}^d$ represent the ground truth labeling function. As a first try, a reference model $f_T : \mathbb{R}^n \rightarrow \mathbb{R}^d$ trained on the target dataset is obtained through optimizing over a function class $f_T \in \mathbb{F}_T$. Now suppose we have a source model $f_S : \mathbb{R}^n \rightarrow \mathbb{R}^m$ pretrained on source data, and we are curious how f_S transfer to the target data \mathcal{D} ?

Knowledge transferability. Given a trainable function $g : \mathbb{R}^m \rightarrow \mathbb{R}^d$, where $g \in \mathbb{G}$ is from a small function class for efficiency purpose, we care about whether f_S can achieve low loss $\mathcal{L}(\cdot; y, \mathcal{D})$, e.g., mean squared error, after stacking with a trainable function g comparing with f_T , i.e.,

$$\min_{g \in \mathbb{G}} \mathcal{L}(g \circ f_S; y, \mathcal{D}) \quad \text{compare with} \quad \mathcal{L}(f_T; y, \mathcal{D}).$$

Clearly, the solution to this optimization problem depends on the choice of \mathbb{G} . We only consider the class of affine functions, which is commonly used in practice. Formally, the problem that is studied in our theory is stated as follows.

Problem 1. *Given a reference model f_T trained on target distribution \mathcal{D} , and a source model f_S pre-trained on source data. Can we predict the best possible performance of the composite function $g \circ f_S$ on \mathcal{D} , where g is from a bounded affine function class, given adversarial transferability between f_S and f_T ?*

2.1 Adversarial Transferability

We use the ℓ_2 -norm to characterize the effectiveness of an attack.

Definition 1 (Virtual Adversarial Attack [46]). *Given a model $f : \mathbb{R}^n \rightarrow \mathbb{R}^d$, the attack on point \mathbf{x} within ϵ -ball is defined as $\arg \max_{\|\delta\| \leq \epsilon} \|f(\mathbf{x}) - f(\mathbf{x} + \delta)\|_2$. As this is intractable in practice, we*

consider the use of the tangent function to approximate the difference:

$$\delta_{f,\epsilon}(\mathbf{x}) = \arg \max_{\|\delta\| \leq \epsilon} \|\nabla f(\mathbf{x})^\top \delta\|_2,$$

where $\nabla f(\mathbf{x}) \in \mathbb{R}^{n \times d}$ is the Jacobian matrix. The ϵ will be dropped in clear context or when it is irrelevant.

To provide a quantitative view of adversarial transferability, we measure it with two metrics τ_1 and τ_2 , defined as follows. Both metrics are in the range of $[0, 1]$, where higher values indicate more adversarial transferability.

Definition 2 (Adversarial Transferability (Angle)). *Given two functions f_1, f_2 , we assume they have the same input dimension, and may have different output dimensions. The Adversarial Transferability (Angle) of f_1 and f_2 at point \mathbf{x} is defined as the squared cosine value of the angle between the two attacks, i.e.,*

$$\tau_1(\mathbf{x}) = \frac{\langle \delta_{f_1}(\mathbf{x}), \delta_{f_2}(\mathbf{x}) \rangle^2}{\|\delta_{f_1}(\mathbf{x})\|_2^2 \cdot \|\delta_{f_2}(\mathbf{x})\|_2^2}.$$

We denote its expected value as $\tau_1 = \mathbb{E}_{\mathbf{x} \sim \mathcal{D}}[\tau_1(\mathbf{x})]$.

Intuitively, τ_1 characterizes the similarity of the two attacks. The higher the cosine similarity, the better they can be attacked together. However, it is not sufficient to fully characterize how good f_S will perform only knowing the angle of two attack directions. For example, it is possible that the two functions have the same gradient direction but different gradient norms everywhere, which makes it impossible for knowledge transfer.

Therefore, we also need information about *deviation* of a function given attacks. We denote the deviation of a function f , given attack $\delta(\mathbf{x})$, as $f(\mathbf{x} + \delta(\mathbf{x})) - f(\mathbf{x})$, and we define its approximation as

$$\Delta_{f,\delta}(\mathbf{x}) = \nabla f(\mathbf{x})^\top \delta(\mathbf{x}). \quad (1)$$

Accordingly, we define another metric to answer the following question: applying f_1 's adversarial attacks on both the models, how much can the deviation of their function value be aligned by affine transformations?

Definition 3 (Adversarial Transferability (Deviation)). *Given two functions f_1, f_2 with the same input dimensions and potentially different output dimensions, the Adversarial Transferability (Deviation) of adversarial attacks from f_1 to f_2 given data distribution \mathcal{D} is defined as*

$$\tau_2^{f_1 \rightarrow f_2} = \frac{\langle 2\Delta_{f_2, \delta_{f_1}} - \mathbf{A}\Delta_{f_1, \delta_{f_1}}, \mathbf{A}\Delta_{f_1, \delta_{f_1}} \rangle_{\mathcal{D}}}{\|\Delta_{f_2, \delta_{f_1}}\|_{\mathcal{D}}^2},$$

where \mathbf{A} is a constant matrix defined as

$$\mathbf{A} = \text{proj}(\mathbb{E}_{\mathbf{x} \sim \mathcal{D}}[\Delta_{f_2, \delta_{f_1}}(\mathbf{x}) \Delta_{f_1, \delta_{f_1}}(\mathbf{x})^\top] (\mathbb{E}_{\mathbf{x} \sim \mathcal{D}}[\Delta_{f_1, \delta_{f_1}}(\mathbf{x}) \Delta_{f_1, \delta_{f_1}}(\mathbf{x})^\top])^\dagger, \frac{\|\Delta_{f_2, \delta_{f_1}}\|_{\mathcal{D}}}{\|\Delta_{f_1, \delta_{f_1}}\|_{\mathcal{D}}}).$$

To have better sense of τ_2 and the relationships with other quantities, we present a simple example for visual illustration in Figure 2. Note that high τ_2 does not necessarily require $\Delta_{f_1, \delta_{f_1}}$ and $\Delta_{f_2, \delta_{f_1}}$ to be the same, but they are similar in the sense of being linearly transformable. We refer to the proof of Proposition 1 at section B in appendix for detailed explanation of τ_2 .

Proposition 1. *Both τ_1 and τ_2 are in $[0, 1]$.*

2.2 Adversarial Transferability Indicating Knowledge Transferability

In this subsection, we will provide our theoretical results. First, to have a better intuition, we will show a special case where the theorems are simplified, i.e., where f_S and f_T are both $\mathbb{R}^n \rightarrow \mathbb{R}$. Then, we present the general case where f_S and f_T are multi-dimensional. Note that their output dimensions are not necessarily the same.

When f_S and f_T are both $\mathbb{R}^n \rightarrow \mathbb{R}$, the τ_1 and τ_2 come out in a surprisingly elegant form. Let us show what the two metrics are to have further intuition on what τ_1 and τ_2 characterize.

First, let us see what the attack is in this case. As function f has one-dimensional output, its gradient is a vector $\nabla f \in \mathbb{R}^n$. Thus,

$$\delta_{f,\epsilon}(x) = \arg \max_{\|\delta\| \leq \epsilon} \|\nabla f(x)^\top \delta\|_2 = \frac{\epsilon \nabla f(x)}{\|\nabla f(x)\|_2}$$

is simply the gradient with its scale normalized. Then, the τ_1 becomes

$$\tau_1(x) = \frac{\langle \nabla f_S(x), \nabla f_T(x) \rangle^2}{\|\nabla f_S(x)\|_2^2 \cdot \|\nabla f_T(x)\|_2^2},$$

which is the squared cosine (angle) between two gradients. For τ_2 , the matrix A degenerates to a scalar constant, which makes τ_2 simpler as well, i.e.,

$$A = \frac{\langle \Delta_{f_T, \delta_{f_S}}, \Delta_{f_S, \delta_{f_S}} \rangle_{\mathcal{D}}}{\|\Delta_{f_S, \delta_{f_S}}\|_{\mathcal{D}}^2}, \quad \text{and} \quad \tau_2^{f_S \rightarrow f_T} = \frac{\langle \Delta_{f_S, \delta_{f_S}}, \Delta_{f_T, \delta_{f_S}} \rangle_{\mathcal{D}}^2}{\|\Delta_{f_S, \delta_{f_S}}\|_{\mathcal{D}}^2 \cdot \|\Delta_{f_T, \delta_{f_S}}\|_{\mathcal{D}}^2}.$$

We can see, in this case τ_2 is interestingly in the same form of the first metric τ_1 . We will simply use τ_2 to denote $\tau_2^{f_S \rightarrow f_T}$ afterwards.

Accordingly, when f_S and f_T are both $\mathbb{R}^n \rightarrow \mathbb{R}$, the result also comes out in an elegant form. In this case, adversarial attacks reflect all the information of the gradients of the two models, enabling τ_1 and τ_2 to encode all the information we need to prove the following theorem.

Theorem 1. *For two functions f_S and f_T that both are $\mathbb{R}^n \rightarrow \mathbb{R}$, there is an affine function $g : \mathbb{R} \rightarrow \mathbb{R}$, such that*

$$\|\nabla f_T - \nabla(g \circ f_S)\|_{\mathcal{D}}^2 = \mathbb{E}_{\mathbf{x} \sim \mathcal{D}} [(1 - \tau_1(\mathbf{x})\tau_2) \|\nabla f_T(\mathbf{x})\|_2^2],$$

where $g(x) = Ax + \text{Const}$. Moreover, if assuming that f_T is L -Lipschitz continuous, i.e., $\|\nabla f_T(\mathbf{x})\|_2 \leq L$ for $\forall \mathbf{x} \in \text{supp}(\mathcal{D})$, we have a more elegant statement:

$$\|\nabla f_T - \nabla(g \circ f_S)\|_{\mathcal{D}}^2 \leq (1 - \tau_1\tau_2)L^2.$$

The theorem suggests that, if adversarial transferability is high, there exists an affine transformation with bounded norm, such that $g \circ f_S$ is close to f_T . As an intuition of the proof, the difference between two gradients can be represented by the angle between them, which can be characterized by τ_1 ; and the norm difference between them, which can be characterized by τ_2 .

Similar to the general case, we consider when the output dimensions of both functions are multi-dimensional and not necessarily the same. In this scenario, adversarial attacks correspond to the largest singular value of the Jacobian matrix. Therefore, we need to introduce the following definition to capture other information that is not revealed by adversarial attacks.

Definition 4 (Singular Value Ratio). *For any function f , the Singular Value Ratio for the function gradient at \mathbf{x} is defined as $\lambda_f(\mathbf{x}) = \frac{\sigma_2(\mathbf{x})}{\sigma_1(\mathbf{x})}$, where $\sigma_1(\mathbf{x}), \sigma_2(\mathbf{x})$ are the largest and the second largest singular value in absolute value of $\nabla f(\mathbf{x})$, respectively. In addition, we define the worst-case singular value ratio as $\lambda_f = \max_{\mathbf{x} \in \text{supp}(\mathcal{D})} \lambda_f(\mathbf{x})$.*

Theorem 2. *For two functions $f_S : \mathbb{R}^n \rightarrow \mathbb{R}^m$, and $f_T : \mathbb{R}^n \rightarrow \mathbb{R}^d$, assuming that f_T is L -Lipschitz continuous, i.e., $\|\nabla f_T(\mathbf{x})\|_2 \leq L$ for $\forall \mathbf{x} \in \text{supp}(\mathcal{D})$, there is an affine function $g : \mathbb{R}^m \rightarrow \mathbb{R}^d$, such that*

$$\|\nabla f_T - \nabla(g \circ f_S)\|_{\mathcal{D}}^2 \leq \left((1 - \tau_1\tau_2) + (1 - \tau_1)(1 - \tau_2)\lambda_{f_T}^2 + (\lambda_{f_T} + \lambda_{f_S})^2 \right) 5L^2,$$

where g is defined as $g(\mathbf{z}) = \mathbf{A}\mathbf{z} + \text{Const}$.

Note that, as Theorem 1, this theorem also has a statement offering tighter bound where we do not assume Lipschitz continuous. The full version of this theorem is provided in appendix. What we have now is a bound on the norms of the gradients. Intuitively, given the right constant value shift, minimal difference in gradients implies minimal difference in function value, which should result in bounded loss. Indeed, we prove that the squared loss of the transferred model $g \circ f_S$ is bounded by the loss of f_T and their gradient difference, by assuming the β -smoothness of both the functions.

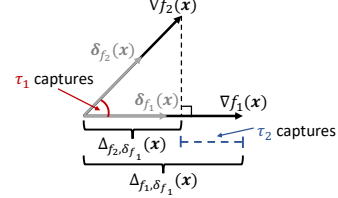


Figure 2: Illustration of all the variables in a case where both f_1, f_2 are $\mathbb{R}^n \rightarrow \mathbb{R}$, and both attacks $\delta_{f_1}(\mathbf{x}), \delta_{f_2}(\mathbf{x})$ are of unit length.

Definition 5 (β -smoothness). A function f is β -smooth if for all \mathbf{x}, \mathbf{y} ,

$$\|\nabla f(\mathbf{x}) - \nabla f(\mathbf{y})\|_2 \leq \beta \|\mathbf{x} - \mathbf{y}\|_2.$$

For the target data distribution \mathcal{D} , and its ground truth labeling function y , the mean squared loss of the transferred model is $\mathbb{E}_{\mathbf{x} \sim \mathcal{D}} \|g \circ f_S(\mathbf{x}) - y(\mathbf{x})\|_2^2 = \|g \circ f_S - y\|_{\mathcal{D}}^2$. Therefore, the following theorem presents upper bound on the mean squared loss of the transferred model.

Theorem 3. *Without loss of generality we assume $\|\mathbf{x}\|_2 \leq 1$ for $\forall \mathbf{x} \in \text{supp}(\mathcal{D})$. Consider functions $f_S : \mathbb{R}^n \rightarrow \mathbb{R}^m$, $f_T : \mathbb{R}^n \rightarrow \mathbb{R}^d$, and an affine function $g : \mathbb{R}^m \rightarrow \mathbb{R}^d$, suggested by Theorem 1 or Theorem 2, with the constant set to let $g(f_S(\mathbf{0})) = f_T(\mathbf{0})$. If both f_T, f_S are β -smooth, then*

$$\|g \circ f_S - y\|_{\mathcal{D}}^2 \leq \left(\|f_T - y\|_{\mathcal{D}} + \|\nabla f_T - \nabla g \circ f_S\|_{\mathcal{D}} + \left(1 + \frac{\|\nabla f_T\|_{\mathcal{D},2}}{\|\nabla f_S\|_{\mathcal{D},2}} \right) \beta \right)^2.$$

3 Characterizing the Knowledge and Adversarial Transferability

Efforts on searching for proper inductive bias can be dated back to the dawn of AI, when Turing argues to use learning elements to construct intelligent systems, instead of building them from the scratch [71]. This idea has had a profound impact and quickly metamorphosized into various forms, including but not limited to, Bayesian inference [36, 69, 68, 17, 18], Few-shot Learning [66, 59, 12, 49, 64], Domain Adaptation [24, 42, 74, 72] and Transfer Learning [53, 6, 85, 43, 50, 7, 67]. In this section, we first summarize the categories of knowledge transferability and then provide a measure for adversarial transferability as a proxy of knowledge transferability in practice.

3.1 Categories of Knowledge Transferability

Transfer Learning focuses on applying the knowledge gained from one problem to another. Specifically, two approaches are most concerned. First, Direct-transfer: only the new output layers' weights are updated, whereas the rest of the network is frozen; Second, Fine-tuning: all weights of the model are updated based on the target problem. To measure the knowledge transferability quantitatively, we follow the convention by computing the final loss of the transferred models [61, 3, 43]. We measure how well adversarial transferability indicates the knowledge transferability in the following scenarios.

Knowledge-transfer among data distributions is the most common setting of transfer learning. It transfers the knowledge of a model trained/gained from one data domain to the other data domains. For instance, Shiel et al. [60] manage to use pre-trained ImageNet representations to achieve state-of-the-art accuracy for medical data analysis. Furthermore, Huh et al. [26] and Kornblith et al. [34] investigate the reasons and conditions for ImageNet to be a good transfer source.

Knowledge-transfer among attributes is a popular method to handle zero-shot and few-shot learning problems [29, 55, 81]. It transfers the knowledge learned from the attributes of the source problem to a new target problem. For instance, Russakovsky et al. [57] build a large scale dataset with attributes to facilitate zero-shot object recognition. Kankuekul et al. [32] even demonstrate that attribute transfer can be done in an online manner.

Knowledge-transfer among tasks is widely applied across various vision tasks, such as super resolution [30], style transfer [13], semantic and instance segmentation [15, 20, 40]. It involves transferring the knowledge the model gains by learning to do one task to another novel task. Although there are doubts [19, 54] about the efficacy of pre-training, it is still the predominant way of getting good performance when the training data of the new task is scarce. Thus, many recent works [1, 65, 82] are dedicated to charting the affinity map between tasks, aiming to guide potential transfer.

3.2 Measurement of Adversarial Transferability

Existing studies have shown that models trained on the same data distribution and architectures share high adversarial transferability [38, 51, 70]. Heo et al. [22] even propose to map function's decision boundary with adversarial examples empirically. Therefore it is natural to ask: *do the models trained on similar but not identical data or tasks still share high adversarial transferability?* To answer this question, we need a generic attack method that can be used to estimate the adversarial transferability between models. However, the optimization problem in Definition 1 is practically hard to solve. So we approximate this process by the effective attack approach PGD [35] with random re-starts.

We measure the adversarial transferability based on PGD attacks in practice. PGD attack is generated iteratively: denote step size as ξ , the source model as f_S , and the loss function on the source problem. $\ell_S(\cdot, \cdot)$. We initialize \mathbf{x}_0 to be uniformly sampled from the ϵ -ball $\mathbb{B}_\epsilon(\mathbf{x})$ of radius ϵ centered as instance \mathbf{x} , and then generate the adversarial instance iteratively: at step t we compute $\mathbf{x}_{t+1} = \mathbf{x}_t + \xi \cdot \text{sign}(\nabla_{\mathbf{x}_t} \ell_S(f_S(\mathbf{x}_t), f_S(\mathbf{x})))$. Denoting the adversarial example at instance \mathbf{x} using PGD on source model f_S as $PGD_{f_S}(\mathbf{x})$, we measure the *empirical adversarial transferability* from f_S to f_T based on the loss $\ell_T(\cdot, y)$ of f_T on target data \mathcal{D} given attacks generated on f_S , i.e.,

$$\mathcal{L}_T(f_T \circ PGD_{f_S}; y, \mathcal{D}) = \mathbb{E}_{\mathbf{x} \sim \mathcal{D}} \ell_T(f_T(PGD_{f_S}(\mathbf{x})), y(\mathbf{x})). \quad (2)$$

In the following, we show its connection with the adversarial transferability defined in our theory.

Proposition 2. *If \mathcal{L}_T is mean squared loss, f_T achieves zero loss, and the attack recovers the virtual adversarial attack within an small ϵ -ball (Definition 1), the empirical adversarial transferability defined in (2) is approximately upper and lower bounded by*

$$\begin{aligned} \mathcal{L}_T(f_T \circ PGD_{f_S}; y, \mathcal{D}) &\geq \epsilon^2 \mathbb{E}_{\mathbf{x} \sim \mathcal{D}} \left[\tau_1(\mathbf{x}) \|\nabla f_T(\mathbf{x})\|_2^2 \right] + O(\epsilon^3), \\ \mathcal{L}_T(f_T \circ PGD_{f_S}; y, \mathcal{D}) &\leq \epsilon^2 \mathbb{E}_{\mathbf{x} \sim \mathcal{D}} \left[(\lambda_{f_T}^2 + (1 - \lambda_{f_T}^2) \tau_1(\mathbf{x})) \|\nabla f_T(\mathbf{x})\|_2^2 \right] + O(\epsilon^3), \end{aligned}$$

where $O(\epsilon^3)$ denotes a cubic error term. We can see that as $\tau_1(\mathbf{x})$ becomes larger, both bounds become larger, i.e., τ_1 and the empirical adversarial transferability are positively correlated.

4 Experimental Evaluation

In this section, we will describe the empirical evaluation of the relationship between adversarial transferability and knowledge transferability in three knowledge transfer scenarios: knowledge transfer on data distributions, attributes, and tasks. Each of the experiments will be presented and discussed in this order. All training details are deferred to the Appendix.

4.1 Adversarial Transferability Indicates Knowledge-transfer among Data Distributions

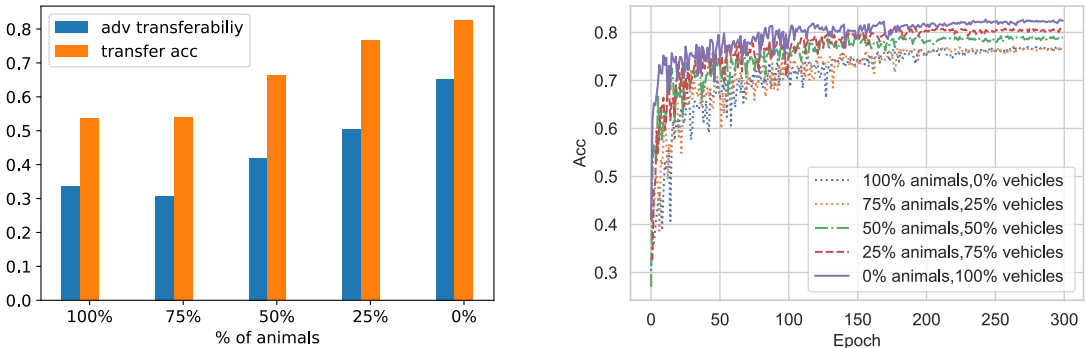


Figure 3: (left): correlation between the adversarial transferability and knowledge ttranserability. (right): models with higher adversarial transferability converge faster in fine-tuning.

This experiment shows that the closer the source data distribution is to the target data distribution, the more adversarially transferable the source model to the reference model, thus we observe that the source model is more knowledge transferable to the target dataset.

Dataset. We manually construct five source datasets (5 source models) based on CIFAR-10 [23] and a single target dataset (1 reference model) based on STL-10 [5]. We divide the classes of the original datasets into two categories, animals (bird, cat, deer, dog) and transportation vehicles (airplane, automobile, ship, truck). Each of the source datasets consists of different a percentage of animals and transportation vehicles, while the target dataset contains only transportation vehicles, which is meant to control the closeness of the two data distributions.

Adversarial Transferability. We take 1000 test images (STL-10) from the target dataset and

generate 1000 adversarial examples on each of the five source models with virtual adversarial attacks as described in section 3. The choices of ϵ (i.e., the L_∞ norm bound) include 0.03, 0.06, 0.1, 0.2. For PGD based attacks, we only run 10 steps for efficiency. We measure the transfer effectiveness of the adversarial examples by computing the cross-entropy loss on the reference model.

Knowledge Transferability. To measure the knowledge transferability, we fine-tune a new linear layer on the target dataset to replace the last layer of each source model to generate the corresponding *transferred models*. Then we measure the performance of the five transferred models on the target dataset based on the standard accuracy and cross-entropy loss.

Results From figure 3 (left), it is clear that the source models trained on a higher percentage of vehicles (target domain) demonstrate higher adversarial transferability and thus higher knowledge transferability. This makes intuitive sense, since the target dataset consists of only vehicles. In addition, the models of higher adversarial transferability (figure 3 right) also converge faster in fine-tuning, indicating easier knowledge transfer training.

4.2 Adversarial Transferability Indicating Knowledge-transfer among Attributes

In addition to the data distributions, we validate our theory on another dimension, attributes. This experiment suggests that the more adversarially transferable the source model of certain attributes is to the reference model, the better the model performs on the target task aiming to learn target attributes.

Dataset CelebA [39] consists of 202,599 face images from 10,177 identities. A reference facial recognition model is trained on this identities. Each image also comes with 40 binary attributes, on which we train 40 source models. Our goal is to test whether source models of *source attributes*, can transfer to perform facial recognition.

Adversarial Transferability We sample 1000 images from CelebA and perform a virtual adversarial attack as described in section 3 on each of the 40 attribute classifiers. Then we measure the adversarial transfer effectiveness of these adversarial examples on the reference facial recognition model.

Knowledge Transferability To fairly assess the knowledge transferability, we test the 40 *transferred models* on 7 well-known facial recognition benchmarks, LFW [25], CFP-FF, CFP-FP [58], AgeDB [47], CALFW, CPLFW [83] and VGG2-FP [4]. We report the classification accuracy separately for each of the target datasets.

Result In figure 4, we list the top-5 attribute source models that share the highest adversarial transferability and the performance of their transferred models on the 7 target facial recognition benchmarks. We observe that the attribute "Young" has the highest adversarial transferability; as a result, it also achieves highest classification performance in 5 out of the 7 benchmarks, while performing decently well in the rest of the 2.

4.3 Adversarial Transferability Indicating Knowledge-transfer among Tasks

In this experiment, we aim to show that adversarial transferability can also indicate the knowledge transferability among different machine learning tasks. Zamir et al. [82] shows that models trained on different tasks can transfer to other tasks well, especially when the tasks belong to the same "category". Here we leverage the same dataset, and pick 15 single image tasks from the task pool, including Autoencoding, 2D Segmentation, 3D Keypoint and etc. Intuitively, these tasks can be categorized into 3 categories, semantic task, 2D tasks as well as 3D tasks. Leveraging the tasks within the same category, which would hypothetically have higher adversarial transferability, we evaluate the corresponding knowledge transferability.

Dataset The Taskonomy-data [82] consists of 4 million images of indoor scenes from about 600

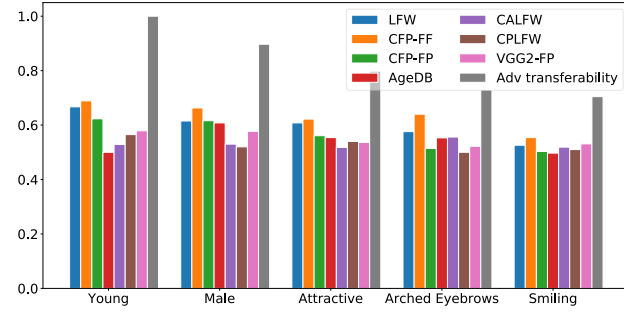


Figure 4: Top 5 Attributes with the highest adversarial transferability and their corresponding performance on each of the validation benchmarks. The adv transferability is normalized to range [0,1] by dividing the largest value. Attributes with lower adversarial transferability observe lower knowledge transferability from the left to right.

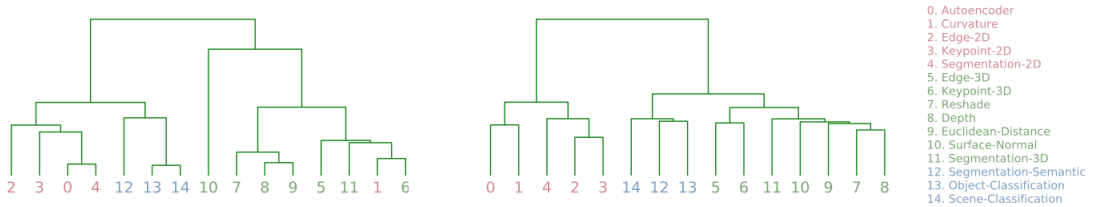


Figure 5: Left: Empirically confirmed taskonomy prediction of task categories [82]. Right: Task category prediction based on adversarial transferability. Different colors represent different task categories including 2D, 3D, Semantic. It is obvious that the adversarial transferability is able to predict similar task categories aligned with the pure knowledge-transfer empirical observation.

indoor images, every one of which has annotations for every task listed in the pool. We use a public subset[82] of these images to validate our theory.

Adversarial Transferability *Adversarial Transferability Matrix (ATM)* is used here to measure the adversarial transferability between multiple tasks, modified from the *Affinity Matrix* in [82]. Detailed definition is deferred to the Appendix. To generate the corresponding “task categories” for comparison, we sample 1000 images from the public dataset and perform a virtual adversarial attack on each of the 15 source models. Adversarial perturbation with ϵ (L_∞ norm) as 0.03, 0.06 are used and we run 10 steps PGD-based attack for efficiency. Then we measure these adversarial examples’ effectiveness on each of the 15 tasks by the corresponding loss functions. After we obtain the 15×15 ATM, we take columns of this matrix as features for each task and perform agglomerative clustering to obtain the Task Similarity Tree.

Knowledge Transferability We use the affinity scores provided as a 15×15 affinity matrix by [82] to compute the categories of tasks. Then we take columns of this matrix as features for each task and perform agglomerative clustering to obtain the Task Similarity Tree.

Result Figure 5 compares the predictions of task categories generated based on adversarial transferability and knowledge transferability in [82]. It is easy to see three intuitive categories are formed, i.e, 2D, 3D, and Semantic tasks for both adversarial and knowledge transferability. To provide a quantitative measurement of the similarity, we also compute the average inner category entropy based on adversarial transferability with the categories in [82] as the ground truth (the lower entropy indicates higher correlation between adversarial and knowledge transferability). In figure 6 (Appendix), the adversarial transferability based category prediction shows low entropy when the number of categories is greater or equal to 3, which indicates that the adversarial transferability is faithful with the category prediction in [82]. This result shows strong positive correlation between the adversarial transferability and knowledge transferability among learning tasks in terms of predicting the similar task categories.

5 Conclusion

We theoretically analyze the relationship between adversarial transferability and knowledge transferability, along with thorough experimental justifications in diverse scenarios. Both our theoretical and empirical results show that adversarial transferability can indicate knowledge transferability, which opens up a new door for assessing and enhancing knowledge-based transfer learning. To further effectively evaluate the adversarial transferability, one possible future direction would be to identify promising pretrained models as reference models, without the overhead of training from scratch.

References

- [1] Alessandro Achille, Michael Lam, Rahul Tewari, Avinash Ravichandran, Subhransu Maji, Charless C Fowlkes, Stefano Soatto, and Pietro Perona. Task2vec: Task embedding for meta-learning. In *Proceedings of the IEEE International Conference on Computer Vision*, pages 6430–6439, 2019.

[2] Anish Athalye, Nicholas Carlini, and David Wagner. Obfuscated gradients give a false sense of security: Circumventing defenses to adversarial examples. In *International Conference on Machine Learning*, pages 274–283, 2018.

[3] Yoshua Bengio. Deep learning of representations for unsupervised and transfer learning. In *Proceedings of ICML workshop on unsupervised and transfer learning*, pages 17–36, 2012.

[4] Q. Cao, L. Shen, W. Xie, O. M. Parkhi, and A. Zisserman. Vggface2: A dataset for recognising faces across pose and age. In *International Conference on Automatic Face and Gesture Recognition*, 2018.

[5] Adam Coates, Andrew Ng, and Honglak Lee. An analysis of single-layer networks in unsupervised feature learning. In *Proceedings of the fourteenth international conference on artificial intelligence and statistics*, pages 215–223, 2011.

[6] Diane Cook, Kyle D Feuz, and Narayanan C Krishnan. Transfer learning for activity recognition: A survey. *Knowledge and information systems*, 36(3):537–556, 2013.

[7] Wenyuan Dai, Qiang Yang, Gui-Rong Xue, and Yong Yu. Boosting for transfer learning. In *Proceedings of the 24th international conference on Machine learning*, pages 193–200, 2007.

[8] Ambra Demontis, Marco Melis, Maura Pintor, Matthew Jagielski, Battista Biggio, Alina Oprea, Cristina Nita-Rotaru, and Fabio Roli. Why do adversarial attacks transfer? explaining transferability of evasion and poisoning attacks. In *28th {USENIX} Security Symposium ({USENIX} Security 19)*, pages 321–338, 2019.

[9] Jiankang Deng, Jia Guo, Niannan Xue, and Stefanos Zafeiriou. Arcface: Additive angular margin loss for deep face recognition. In *Proceedings of the IEEE Conference on Computer Vision and Pattern Recognition*, pages 4690–4699, 2019.

[10] Jacob Devlin, Ming-Wei Chang, Kenton Lee, and Kristina Toutanova. Bert: Pre-training of deep bidirectional transformers for language understanding. *arXiv preprint arXiv:1810.04805*, 2018.

[11] Yinpeng Dong, Tianyu Pang, Hang Su, and Jun Zhu. Evading defenses to transferable adversarial examples by translation-invariant attacks. In *Proceedings of the IEEE Conference on Computer Vision and Pattern Recognition*, pages 4312–4321, 2019.

[12] Li Fei-Fei et al. A bayesian approach to unsupervised one-shot learning of object categories. In *Proceedings Ninth IEEE International Conference on Computer Vision*, pages 1134–1141. IEEE, 2003.

[13] Leon A Gatys, Alexander S Ecker, and Matthias Bethge. Image style transfer using convolutional neural networks. In *Proceedings of the IEEE conference on computer vision and pattern recognition*, pages 2414–2423, 2016.

[14] Robert Geirhos, Patricia Rubisch, Claudio Michaelis, Matthias Bethge, Felix A Wichmann, and Wieland Brendel. Imagenet-trained cnns are biased towards texture; increasing shape bias improves accuracy and robustness. *arXiv preprint arXiv:1811.12231*, 2018.

[15] Ross Girshick. Fast r-cnn. In *Proceedings of the IEEE international conference on computer vision*, pages 1440–1448, 2015.

[16] Ian J Goodfellow, Jonathon Shlens, and Christian Szegedy. Explaining and harnessing adversarial examples. *arXiv preprint arXiv:1412.6572*, 2014.

[17] Alison Gopnik, Clark Glymour, David M Sobel, Laura E Schulz, Tamar Kushnir, and David Danks. A theory of causal learning in children: causal maps and bayes nets. *Psychological review*, 111(1):3, 2004.

[18] Alison Gopnik, Andrew N Meltzoff, and Patricia K Kuhl. *The scientist in the crib: Minds, brains, and how children learn*. William Morrow & Co, 1999.

[19] Kaiming He, Ross Girshick, and Piotr Dollár. Rethinking imagenet pre-training. In *Proceedings of the IEEE International Conference on Computer Vision*, pages 4918–4927, 2019.

[20] Kaiming He, Georgia Gkioxari, Piotr Dollár, and Ross Girshick. Mask r-cnn. In *Proceedings of the IEEE international conference on computer vision*, pages 2961–2969, 2017.

[21] Kaiming He, Xiangyu Zhang, Shaoqing Ren, and Jian Sun. Identity mappings in deep residual networks. In *European conference on computer vision*, pages 630–645. Springer, 2016.

[22] Byeongho Heo, Minsik Lee, Sangdoo Yun, and Jin Young Choi. Knowledge distillation with adversarial samples supporting decision boundary. In *Proceedings of the AAAI Conference on Artificial Intelligence*, volume 33, pages 3771–3778, 2019.

[23] Geoffrey E Hinton, Nitish Srivastava, Alex Krizhevsky, Ilya Sutskever, and Ruslan R Salakhutdinov. Improving neural networks by preventing co-adaptation of feature detectors. *arXiv preprint arXiv:1207.0580*, 2012.

[24] Judy Hoffman, Trevor Darrell, and Kate Saenko. Continuous manifold based adaptation for evolving visual domains. In *Proceedings of the IEEE Conference on Computer Vision and Pattern Recognition*, pages 867–874, 2014.

[25] Gary B. Huang, Manu Ramesh, Tamara Berg, and Erik Learned-Miller. Labeled faces in the wild: A database for studying face recognition in unconstrained environments. Technical Report 07-49, University of Massachusetts, Amherst, October 2007.

[26] Minyoung Huh, Pulkit Agrawal, and Alexei A Efros. What makes imagenet good for transfer learning? *arXiv preprint arXiv:1608.08614*, 2016.

[27] Andrew Ilyas, Logan Engstrom, Anish Athalye, and Jessy Lin. Black-box adversarial attacks with limited queries and information. In *International Conference on Machine Learning*, pages 2137–2146, 2018.

[28] Andrew Ilyas, Shibani Santurkar, Dimitris Tsipras, Logan Engstrom, Brandon Tran, and Aleksander Madry. Adversarial examples are not bugs, they are features. In *Advances in Neural Information Processing Systems*, pages 125–136, 2019.

[29] Dinesh Jayaraman and Kristen Grauman. Zero-shot recognition with unreliable attributes. In *Advances in neural information processing systems*, pages 3464–3472, 2014.

[30] Justin Johnson, Alexandre Alahi, and Li Fei-Fei. Perceptual losses for real-time style transfer and super-resolution. In *European conference on computer vision*, pages 694–711. Springer, 2016.

[31] Seong Joon Oh, Mario Fritz, and Bernt Schiele. Adversarial image perturbation for privacy protection—a game theory perspective. In *Proceedings of the IEEE International Conference on Computer Vision*, pages 1482–1491, 2017.

[32] Pichai Kankuekul, Aram Kawewong, Sirinart Tangruamsub, and Osamu Hasegawa. Online incremental attribute-based zero-shot learning. In *2012 IEEE Conference on Computer Vision and Pattern Recognition*, pages 3657–3664. IEEE, 2012.

[33] Jiman Kim and Chanjong Park. End-to-end ego lane estimation based on sequential transfer learning for self-driving cars. In *Proceedings of the IEEE Conference on Computer Vision and Pattern Recognition Workshops*, pages 30–38, 2017.

[34] Simon Kornblith, Jonathon Shlens, and Quoc V Le. Do better imagenet models transfer better? In *Proceedings of the IEEE conference on computer vision and pattern recognition*, pages 2661–2671, 2019.

[35] Alexey Kurakin, Ian Goodfellow, and Samy Bengio. Adversarial machine learning at scale. *arXiv preprint arXiv:1611.01236*, 2016.

[36] Brenden M Lake, Ruslan Salakhutdinov, and Joshua B Tenenbaum. Human-level concept learning through probabilistic program induction. *Science*, 350(6266):1332–1338, 2015.

[37] Tsung-Yi Lin, Priya Goyal, Ross Girshick, Kaiming He, and Piotr Dollár. Focal loss for dense object detection. In *Proceedings of the IEEE international conference on computer vision*, pages 2980–2988, 2017.

[38] Yanpei Liu, Xinyun Chen, Chang Liu, and Dawn Song. Delving into transferable adversarial examples and black-box attacks. *arXiv preprint arXiv:1611.02770*, 2016.

[39] Ziwei Liu, Ping Luo, Xiaogang Wang, and Xiaoou Tang. Large-scale celebfaces attributes (celeba) dataset. *Retrieved August*, 15:2018, 2018.

[40] Jonathan Long, Evan Shelhamer, and Trevor Darrell. Fully convolutional networks for semantic segmentation. In *Proceedings of the IEEE conference on computer vision and pattern recognition*, pages 3431–3440, 2015.

[41] Mingsheng Long, Yue Cao, Jianmin Wang, and Michael Jordan. Learning transferable features with deep adaptation networks. In *International Conference on Machine Learning*, pages 97–105, 2015.

[42] Mingsheng Long, Han Zhu, Jianmin Wang, and Michael I Jordan. Unsupervised domain adaptation with residual transfer networks. In *Advances in neural information processing systems*, pages 136–144, 2016.

[43] Mingsheng Long, Han Zhu, Jianmin Wang, and Michael I Jordan. Deep transfer learning with joint adaptation networks. In *Proceedings of the 34th International Conference on Machine Learning-Volume 70*, pages 2208–2217. JMLR. org, 2017.

[44] Xingjun Ma, Bo Li, Yisen Wang, Sarah M Erfani, Sudanthi Wijewickrema, Grant Schoenebeck, Dawn Song, Michael E Houle, and James Bailey. Characterizing adversarial subspaces using local intrinsic dimensionality. *arXiv preprint arXiv:1801.02613*, 2018.

[45] Ana I Maqueda, Antonio Loquercio, Guillermo Gallego, Narciso García, and Davide Scaramuzza. Event-based vision meets deep learning on steering prediction for self-driving cars. In *Proceedings of the IEEE Conference on Computer Vision and Pattern Recognition*, pages 5419–5427, 2018.

[46] Takeru Miyato, Shin-ichi Maeda, Masanori Koyama, and Shin Ishii. Virtual adversarial training: a regularization method for supervised and semi-supervised learning. *IEEE transactions on pattern analysis and machine intelligence*, 41(8):1979–1993, 2018.

[47] Stylianos Moschoglou, Athanasios Papaioannou, Christos Sagonas, Jiankang Deng, Irene Kotsia, and Stefanos Zafeiriou. Agedb: the first manually collected, in-the-wild age database. In *Proceedings of the IEEE Conference on Computer Vision and Pattern Recognition Workshop*, volume 2, page 5, 2017.

[48] Muhammad Muzammal Naseer, Salman H Khan, Muhammad Haris Khan, Fahad Shahbaz Khan, and Fatih Porikli. Cross-domain transferability of adversarial perturbations. In *Advances in Neural Information Processing Systems*, pages 12885–12895, 2019.

[49] Mohammad Norouzi, Tomas Mikolov, Samy Bengio, Yoram Singer, Jonathon Shlens, Andrea Frome, Greg S Corrado, and Jeffrey Dean. Zero-shot learning by convex combination of semantic embeddings. *arXiv preprint arXiv:1312.5650*, 2013.

[50] Sinno Jialin Pan and Qiang Yang. A survey on transfer learning. *IEEE Transactions on knowledge and data engineering*, 22(10):1345–1359, 2009.

[51] Nicolas Papernot, Patrick McDaniel, and Ian Goodfellow. Transferability in machine learning: from phenomena to black-box attacks using adversarial samples. *arXiv preprint arXiv:1605.07277*, 2016.

[52] Nicolas Papernot, Patrick McDaniel, Ian Goodfellow, Somesh Jha, Z Berkay Celik, and Ananthram Swami. Practical black-box attacks against machine learning. In *Proceedings of the 2017 ACM on Asia conference on computer and communications security*, pages 506–519, 2017.

[53] Lorien Y Pratt. Discriminability-based transfer between neural networks. In *Advances in neural information processing systems*, pages 204–211, 1993.

[54] Benjamin Recht, Rebecca Roelofs, Ludwig Schmidt, and Vaishaal Shankar. Do imagenet classifiers generalize to imagenet? In *International Conference on Machine Learning*, pages 5389–5400, 2019.

[55] Bernardino Romera-Paredes and Philip Torr. An embarrassingly simple approach to zero-shot learning. In *International Conference on Machine Learning*, pages 2152–2161, 2015.

[56] Olga Russakovsky, Jia Deng, Hao Su, Jonathan Krause, Sanjeev Satheesh, Sean Ma, Zhiheng Huang, Andrej Karpathy, Aditya Khosla, Michael Bernstein, et al. Imagenet large scale visual recognition challenge. *International journal of computer vision*, 115(3):211–252, 2015.

[57] Olga Russakovsky and Li Fei-Fei. Attribute learning in large-scale datasets. In *European Conference on Computer Vision*, pages 1–14. Springer, 2010.

[58] C.D. Castillo V.M. Patel R. Chellappa D.W. Jacobs S. Sengupta, J.C. Cheng. Frontal to profile face verification in the wild. In *IEEE Conference on Applications of Computer Vision*, February 2016.

[59] Ruslan Salakhutdinov, Joshua Tenenbaum, and Antonio Torralba. One-shot learning with a hierarchical nonparametric bayesian model. In *Proceedings of ICML Workshop on Unsupervised and Transfer Learning*, pages 195–206, 2012.

[60] Chuen-Kai Shie, Chung-Hisang Chuang, Chun-Nan Chou, Meng-Hsi Wu, and Edward Y Chang. Transfer representation learning for medical image analysis. In *2015 37th annual international conference of the IEEE Engineering in Medicine and Biology Society (EMBC)*, pages 711–714. IEEE, 2015.

[61] Hoo-Chang Shin, Holger R Roth, Mingchen Gao, Le Lu, Ziyue Xu, Isabella Nogues, Jianhua Yao, Daniel Mollura, and Ronald M Summers. Deep convolutional neural networks for computer-aided detection: Cnn architectures, dataset characteristics and transfer learning. *IEEE transactions on medical imaging*, 35(5):1285–1298, 2016.

[62] Yosuke Shinya, Edgar Simo-Serra, and Taiji Suzuki. Understanding the effects of pre-training for object detectors via eigenspectrum. In *Proceedings of the IEEE International Conference on Computer Vision Workshops*, pages 0–0, 2019.

[63] Karen Simonyan and Andrew Zisserman. Very deep convolutional networks for large-scale image recognition. *arXiv preprint arXiv:1409.1556*, 2014.

[64] Richard Socher, Milind Ganjoo, Christopher D Manning, and Andrew Ng. Zero-shot learning through cross-modal transfer. In *Advances in neural information processing systems*, pages 935–943, 2013.

[65] Trevor Standley, Amir R Zamir, Dawn Chen, Leonidas Guibas, Jitendra Malik, and Silvio Savarese. Which tasks should be learned together in multi-task learning? *arXiv preprint arXiv:1905.07553*, 2019.

[66] Qianru Sun, Yaoyao Liu, Tat-Seng Chua, and Bernt Schiele. Meta-transfer learning for few-shot learning. In *Proceedings of the IEEE Conference on Computer Vision and Pattern Recognition*, pages 403–412, 2019.

[67] Matthew E Taylor and Peter Stone. Transfer learning for reinforcement learning domains: A survey. *Journal of Machine Learning Research*, 10(Jul):1633–1685, 2009.

[68] Joshua B Tenenbaum and Thomas L Griffiths. Generalization, similarity, and bayesian inference. *Behavioral and brain sciences*, 24(4):629–640, 2001.

[69] Joshua B Tenenbaum, Charles Kemp, Thomas L Griffiths, and Noah D Goodman. How to grow a mind: Statistics, structure, and abstraction. *science*, 331(6022):1279–1285, 2011.

[70] Florian Tramèr, Nicolas Papernot, Ian Goodfellow, Dan Boneh, and Patrick McDaniel. The space of transferable adversarial examples. *arXiv preprint arXiv:1704.03453*, 2017.

[71] Alan M Turing. Computing machinery and intelligence. In *Parsing the Turing Test*, pages 23–65. Springer, 2009.

[72] Eric Tzeng, Judy Hoffman, Kate Saenko, and Trevor Darrell. Adversarial discriminative domain adaptation. In *Proceedings of the IEEE Conference on Computer Vision and Pattern Recognition*, pages 7167–7176, 2017.

[73] Annegreet Van Opbroek, M Arfan Ikram, Meike W Vernooij, and Marleen De Brujne. Transfer learning improves supervised image segmentation across imaging protocols. *IEEE transactions on medical imaging*, 34(5):1018–1030, 2014.

[74] Hemanth Venkateswara, Jose Eusebio, Shayok Chakraborty, and Sethuraman Panchanathan. Deep hashing network for unsupervised domain adaptation. In *Proceedings of the IEEE Conference on Computer Vision and Pattern Recognition*, pages 5018–5027, 2017.

[75] Weiyue Wang, Naiyan Wang, Xiaomin Wu, Suya You, and Ulrich Neumann. Self-paced cross-modality transfer learning for efficient road segmentation. In *2017 IEEE International Conference on Robotics and Automation (ICRA)*, pages 1394–1401. IEEE, 2017.

[76] Zirui Wang, Zihang Dai, Barnabás Póczos, and Jaime Carbonell. Characterizing and avoiding negative transfer. In *Proceedings of the IEEE Conference on Computer Vision and Pattern Recognition*, pages 11293–11302, 2019.

[77] Michael Wurm, Thomas Stark, Xiao Xiang Zhu, Matthias Weigand, and Hannes Taubenböck. Semantic segmentation of slums in satellite images using transfer learning on fully convolutional neural networks. *ISPRS journal of photogrammetry and remote sensing*, 150:59–69, 2019.

- [78] Cihang Xie, Zhishuai Zhang, Yuyin Zhou, Song Bai, Jianyu Wang, Zhou Ren, and Alan L Yuille. Improving transferability of adversarial examples with input diversity. In *Proceedings of the IEEE Conference on Computer Vision and Pattern Recognition*, pages 2730–2739, 2019.
- [79] Ruijia Xu, Guanbin Li, Jihan Yang, and Liang Lin. Larger norm more transferable: An adaptive feature norm approach for unsupervised domain adaptation. In *Proceedings of the IEEE International Conference on Computer Vision*, pages 1426–1435, 2019.
- [80] Jason Yosinski, Jeff Clune, Yoshua Bengio, and Hod Lipson. How transferable are features in deep neural networks? In *Advances in neural information processing systems*, pages 3320–3328, 2014.
- [81] Xiaodong Yu and Yiannis Aloimonos. Attribute-based transfer learning for object categorization with zero/one training example. In *European conference on computer vision*, pages 127–140. Springer, 2010.
- [82] Amir R Zamir, Alexander Sax, William Shen, Leonidas J Guibas, Jitendra Malik, and Silvio Savarese. Taskonomy: Disentangling task transfer learning. In *Proceedings of the IEEE Conference on Computer Vision and Pattern Recognition*, pages 3712–3722, 2018.
- [83] Tianyue Zheng, Weihong Deng, and Jian Hu. Cross-age LFW: A database for studying cross-age face recognition in unconstrained environments. *CoRR*, abs/1708.08197, 2017.
- [84] Wen Zhou, Xin Hou, Yongjun Chen, Mengyun Tang, Xiangqi Huang, Xiang Gan, and Yong Yang. Transferable adversarial perturbations. In *Proceedings of the European Conference on Computer Vision (ECCV)*, pages 452–467, 2018.
- [85] Yin Zhu, Yuqiang Chen, Zhongqi Lu, Sinno Jialin Pan, Gui-Rong Xue, Yong Yu, and Qiang Yang. Heterogeneous transfer learning for image classification. In *Twenty-Fifth AAAI Conference on Artificial Intelligence*, 2011.

A Discussion about Validness of the Notations

Before starting proving our theory, it is necessary to show that our mathematical tools are indeed valid. It is easy to verify that $\langle \cdot, \cdot \rangle_{\mathcal{D}}$ is a valid inner product inherited from standard Euclidean inner product. Therefore, the norm $\|\cdot\|_{\mathcal{D}}$, induced by the inner product, is also a valid norm.

What does not come directly is the validness of the norm $\|\cdot\|_{\mathcal{D},2}$. Particularly, whether it satisfies the triangle inequality. Recall that, for a function of matrix output $F : \text{supp}(\mathcal{D}) \rightarrow \mathbb{R}^{d \times m}$, its $L^2(\mathcal{D})$ -norm in accordance with matrix 2-norm is defined as

$$\|F\|_{\mathcal{D},2} = \sqrt{\mathbb{E}_{\mathbf{x} \sim \mathcal{D}} \|F(\mathbf{x})\|_2^2}.$$

For two functions F, G , both are $\text{supp}(\mathcal{D}) \rightarrow \mathbb{R}^{d \times m}$, we can verify the norm $\|\cdot\|_{\mathcal{D},2}$ satisfies triangle inequality as shown in the following. Applying the triangle inequality of the spectral norm, and with some algebra manipulation, it holds that

$$\begin{aligned} \|F + G\|_{\mathcal{D},2} &= \sqrt{\mathbb{E}_{\mathbf{x} \sim \mathcal{D}} \|F(\mathbf{x}) + G(\mathbf{x})\|_2^2} \\ &\leq \sqrt{\mathbb{E}_{\mathbf{x} \sim \mathcal{D}} (\|F(\mathbf{x})\|_2 + \|G(\mathbf{x})\|_2)^2} \\ &= \sqrt{\mathbb{E}_{\mathbf{x} \sim \mathcal{D}} \|F(\mathbf{x})\|_2^2 + \mathbb{E}_{\mathbf{x} \sim \mathcal{D}} \|G(\mathbf{x})\|_2^2 + 2\mathbb{E}_{\mathbf{x} \sim \mathcal{D}} \|F(\mathbf{x})\|_2 \|G(\mathbf{x})\|_2} \\ &= \sqrt{\|F\|_{\mathcal{D},2}^2 + \|G\|_{\mathcal{D},2}^2 + 2\mathbb{E}_{\mathbf{x} \sim \mathcal{D}} \|F(\mathbf{x})\|_2 \|G(\mathbf{x})\|_2}. \end{aligned} \quad (3)$$

Applying the Cauchy-Schwarz inequality, we can see that

$$\begin{aligned} \mathbb{E}_{\mathbf{x} \sim \mathcal{D}} \|F(\mathbf{x})\|_2 \|G(\mathbf{x})\|_2 &\leq \sqrt{\mathbb{E}_{\mathbf{x} \sim \mathcal{D}} \|F(\mathbf{x})\|_2^2 \cdot \mathbb{E}_{\mathbf{x} \sim \mathcal{D}} \|G(\mathbf{x})\|_2^2} \\ &= \|F\|_{\mathcal{D},2} \cdot \|G\|_{\mathcal{D},2}. \end{aligned}$$

Plugging this into (3) would complete the proof, i.e.,

$$\begin{aligned} (3) &\leq \sqrt{\|F\|_{\mathcal{D},2}^2 + \|G\|_{\mathcal{D},2}^2 + 2\|F\|_{\mathcal{D},2} \cdot \|G\|_{\mathcal{D},2}} \\ &= \sqrt{(\|F\|_{\mathcal{D},2} + \|G\|_{\mathcal{D},2})^2} \\ &= \|F\|_{\mathcal{D},2} + \|G\|_{\mathcal{D},2}. \end{aligned}$$

B Proof of Proposition 1

Proposition 1 (Restated). *Both τ_1 and τ_2 are in $[0, 1]$.*

Proof. We are to prove that τ_1 and τ_2 are both in the range of $[0, 1]$. As τ_1 is squared cosine, it is trivial that $\tau_1 \in [0, 1]$. Therefore, we will focus on τ_2 in the following.

Recall that the τ_2 from f_1 to f_2 is defined as

$$\tau_2^{f_1 \rightarrow f_2} = \frac{\langle 2\Delta_{f_2, \delta_{f_1}} - A\Delta_{f_1, \delta_{f_1}}, A\Delta_{f_1, \delta_{f_1}} \rangle_{\mathcal{D}}}{\|\Delta_{f_2, \delta_{f_1}}\|_{\mathcal{D}}^2},$$

where A is a constant matrix defined as

$$A = \text{proj}(\mathbb{E}_{\mathbf{x} \sim \mathcal{D}} [\Delta_{f_2, \delta_{f_1}}(\mathbf{x}) \Delta_{f_1, \delta_{f_1}}(\mathbf{x})^\top] (\mathbb{E}_{\mathbf{x} \sim \mathcal{D}} [\Delta_{f_1, \delta_{f_1}}(\mathbf{x}) \Delta_{f_1, \delta_{f_1}}(\mathbf{x})^\top])^\dagger, \frac{\|\Delta_{f_2, \delta_{f_1}}\|_{\mathcal{D}}}{\|\Delta_{f_1, \delta_{f_1}}\|_{\mathcal{D}}}).$$

For notation convenience, we will simply use τ_2 to denote $\tau_2^{f_1 \rightarrow f_2}$ in this proof.

τ_2 characterizes how similar are the changes in both the function values of $f_1 : \mathbb{R}^n \rightarrow \mathbb{R}^m$ and $f_2 : \mathbb{R}^n \rightarrow \mathbb{R}^d$ in the sense of linear transformable, given attack generated on f_1 . That is being said, it is associated to the function below, i.e.,

$$h(\mathbf{B}) = \|\Delta_{f_2, \delta_{f_1}} - \mathbf{B}\Delta_{f_1, \delta_{f_1}}\|_{\mathcal{D}}^2 = \mathbb{E}_{\mathbf{x} \sim \mathcal{D}} \|\Delta_{f_2, \delta_{f_1}}(\mathbf{x}) - \mathbf{B}\Delta_{f_1, \delta_{f_1}}(\mathbf{x})\|_2^2,$$

where $\Delta_{f_1, \delta_{f_1}} \in \mathbb{R}^m$, $\Delta_{f_2, \delta_{f_1}} \in \mathbb{R}^d$, and $\mathbf{B} \in \mathbb{R}^{d \times m}$.

As $\|\Delta_{f_2, \delta_{f_1}}(\mathbf{x}) - \mathbf{B}\Delta_{f_1, \delta_{f_1}}(\mathbf{x})\|_2^2$ is convex with respect to \mathbf{B} , its expectation, i.e. $h(\mathbf{B})$, is also convex.

Therefore, $h(\mathbf{B})$ it achieves global minima when $\frac{\partial h}{\partial \mathbf{B}} = 0$.

$$\begin{aligned} \frac{\partial h}{\partial \mathbf{B}} &= \mathbb{E}_{\mathbf{x} \sim \mathcal{D}} \frac{\partial}{\partial \mathbf{B}} \left(\|\Delta_{f_2, \delta_{f_1}}(\mathbf{x}) - \mathbf{B}\Delta_{f_1, \delta_{f_1}}(\mathbf{x})\|_2^2 \right) \\ &= 2\mathbb{E}_{\mathbf{x} \sim \mathcal{D}} [(\mathbf{B}\Delta_{f_1, \delta_{f_1}}(\mathbf{x}) - \Delta_{f_2, \delta_{f_1}}(\mathbf{x})) \Delta_{f_1, \delta_{f_1}}(\mathbf{x})^\top] \\ &= 2\mathbb{E}_{\mathbf{x} \sim \mathcal{D}} [\mathbf{B}\Delta_{f_1, \delta_{f_1}}(\mathbf{x}) \Delta_{f_1, \delta_{f_1}}(\mathbf{x})^\top - \Delta_{f_2, \delta_{f_1}}(\mathbf{x}) \Delta_{f_1, \delta_{f_1}}(\mathbf{x})^\top] \\ &= 2\mathbb{E}_{\mathbf{x} \sim \mathcal{D}} [\Delta_{f_1, \delta_{f_1}}(\mathbf{x}) \Delta_{f_1, \delta_{f_1}}(\mathbf{x})^\top] - 2\mathbb{E}_{\mathbf{x} \sim \mathcal{D}} [\Delta_{f_2, \delta_{f_1}}(\mathbf{x}) \Delta_{f_1, \delta_{f_1}}(\mathbf{x})^\top]. \end{aligned}$$

Letting $\frac{\partial h}{\partial \mathbf{B}} = 0$, and denoting the solution as \mathbf{B}^* , we have

$$\mathbf{B}^* = \mathbb{E}_{\mathbf{x} \sim \mathcal{D}} [\Delta_{f_2, \delta_{f_1}}(\mathbf{x}) \Delta_{f_1, \delta_{f_1}}(\mathbf{x})^\top] (\mathbb{E}_{\mathbf{x} \sim \mathcal{D}} [\Delta_{f_1, \delta_{f_1}}(\mathbf{x}) \Delta_{f_1, \delta_{f_1}}(\mathbf{x})^\top])^\dagger.$$

Noting that $\mathbf{A} = \text{proj}(\mathbf{B}^*, \frac{\|\Delta_{f_2, \delta_{f_1}}\|_{\mathcal{D}}}{\|\Delta_{f_1, \delta_{f_1}}\|_{\mathcal{D}}})$ is scaled \mathbf{B}^* , we denote $\mathbf{A} = \psi \mathbf{B}^*$, where ψ a scaling factor depending on \mathbf{B}^* and $\frac{\|\Delta_{f_2, \delta_{f_1}}\|_{\mathcal{D}}}{\|\Delta_{f_1, \delta_{f_1}}\|_{\mathcal{D}}}$. According to the definition of the projection operator, we can see that $0 < \psi \leq 1$.

Replacing \mathbf{B} by \mathbf{A} we have,

$$\begin{aligned} h(\mathbf{A}) &= \|\Delta_{f_2, \delta_{f_1}} - \mathbf{A}\Delta_{f_1, \delta_{f_1}}\|_{\mathcal{D}}^2 = \langle \Delta_{f_2, \delta_{f_1}} - \mathbf{A}\Delta_{f_1, \delta_{f_1}}, \Delta_{f_2, \delta_{f_1}} - \mathbf{A}\Delta_{f_1, \delta_{f_1}} \rangle_{\mathcal{D}} \\ &= \|\Delta_{f_2, \delta_{f_1}}\|_{\mathcal{D}}^2 - \langle 2\Delta_{f_2, \delta_{f_1}} - \mathbf{A}\Delta_{f_1, \delta_{f_1}}, \mathbf{A}\Delta_{f_1, \delta_{f_1}} \rangle_{\mathcal{D}} \\ &= (1 - \tau_2) \|\Delta_{f_2, \delta_{f_1}}\|_{\mathcal{D}}^2. \end{aligned}$$

It is obvious that $h(\mathbf{A}) = \|\Delta_{f_2, \delta_{f_1}} - \mathbf{A}\Delta_{f_1, \delta_{f_1}}\|_{\mathcal{D}}^2 \geq 0$, thus we have $\tau_2 \leq 1$.

As for the lower bound for τ_2 , we will need to use properties of \mathbf{B} . Denoting \mathbf{O} as an all-zero matrix, it holds that

$$h(\mathbf{B}^*) = \min_{\mathbf{B}} \{h(\mathbf{B})\} \leq h(\mathbf{O}). \quad (4)$$

For $\mathbf{A} = \psi \mathbf{B}^*$, according to the convexity of $h(\cdot)$ and the fact that $\psi \in [0, 1]$, we can see the following, i.e.,

$$h(\mathbf{A}) = h(\psi \mathbf{B}^*) = h(\psi \mathbf{B}^* + (1 - \psi) \mathbf{O}) \leq \psi h(\mathbf{B}^*) + (1 - \psi) h(\mathbf{O}).$$

Applying (4) to the above, we can see that

$$h(\mathbf{A}) \leq h(\mathbf{O}).$$

Noting that $h(\mathbf{A}) = (1 - \tau_2) \|\Delta_{f_2, \delta_{f_1}}\|_{\mathcal{D}}^2$ and $h(\mathbf{O}) = \|\Delta_{f_2, \delta_{f_1}}\|_{\mathcal{D}}^2$, the above inequality suggests that

$$\begin{aligned} (1 - \tau_2) \|\Delta_{f_2, \delta_{f_1}}\|_{\mathcal{D}}^2 &\leq \|\Delta_{f_2, \delta_{f_1}}\|_{\mathcal{D}}^2, \\ 0 &\leq \tau_2. \end{aligned}$$

Therefore, τ_2 is upper bounded by 1 and lower bounded by 0. \square

C Proof of Theorem 1

Before actually proving the theorem, let us have a look at what τ_1 and τ_2 are in the case where f_S and f_T are both $\mathbb{R}^n \rightarrow \mathbb{R}$. In this case, both τ_1 and τ_2 come out in an elegant form. Let us show what the two metrics are to have further intuition on what τ_1 and τ_2 characterize.

First, let us see what the attack is in this case. As function f has one-dimensional output, its gradient is a vector $\nabla f \in \mathbb{R}^n$. Thus,

$$\delta_{f,\epsilon}(x) = \arg \max_{\|\delta\| \leq \epsilon} \|\nabla f(x)^\top \delta\|_2 = \frac{\epsilon \nabla f(x)}{\|\nabla f(x)\|_2}$$

Then, the τ_1 becomes

$$\tau_1(x) = \frac{\langle \nabla f_S(x), \nabla f_T(x) \rangle^2}{\|\nabla f_S(x)\|_2^2 \cdot \|\nabla f_T(x)\|_2^2}$$

which is the squared cosine (angle) between two gradients.

For τ_2 , the matrix A degenerates to a scalar constant

$$A = \frac{\langle \Delta_{f_T, \delta_{f_S}}, \Delta_{f_S, \delta_{f_S}} \rangle_{\mathcal{D}}}{\|\Delta_{f_S, \delta_{f_S}}\|_{\mathcal{D}}^2},$$

and the second metric becomes

$$\tau_2^{f_S \rightarrow f_T} = \frac{\langle \Delta_{f_S, \delta_{f_S}}, \Delta_{f_T, \delta_{f_S}} \rangle_{\mathcal{D}}^2}{\|\Delta_{f_S, \delta_{f_S}}\|_{\mathcal{D}}^2 \cdot \|\Delta_{f_T, \delta_{f_S}}\|_{\mathcal{D}}^2}$$

We can see, it is interestingly in the same form of the first metric τ_1 . We will simply use τ_2 to denote $\tau_2^{f_S \rightarrow f_T}$ afterwards.

Theorem 1 (Restated). *For two functions f_S and f_T that both are $\mathbb{R}^n \rightarrow \mathbb{R}$, there is an affine function $g : \mathbb{R} \rightarrow \mathbb{R}$, so that*

$$\|\nabla f_T - \nabla(g \circ f_S)\|_{\mathcal{D}}^2 = \mathbb{E}_{x \sim \mathcal{D}} [(1 - \tau_1(x)\tau_2) \|\nabla f_T(x)\|_2^2],$$

where g is defined as $g(x) = Ax + \text{Const}$.

Moreover, if assuming that f_T is L -Lipschitz continuous, i.e., $\|\nabla f_T(x)\|_2 \leq L$ for $\forall x \in \text{supp}(\mathcal{D})$, we can have a more elegant statement:

$$\|\nabla f_T - \nabla(g \circ f_S)\|_{\mathcal{D}}^2 \leq (1 - \tau_1 \tau_2) L^2.$$

Proof. In the case where g is a one-dimensional affine function, we write is as $g(z) = Az + b$, where A is defined in the definition of τ_2 (Definition 3). In this case, it enjoys a simple form of

$$A = \frac{\langle \Delta_{f_T, \delta_{f_S}}, \Delta_{f_S, \delta_{f_S}} \rangle_{\mathcal{D}}}{\|\Delta_{f_S, \delta_{f_S}}\|_{\mathcal{D}}^2}.$$

Then, we can see that

$$\begin{aligned} \|\nabla f_T - \nabla(g \circ f_S)\|_{\mathcal{D}}^2 &= \|\nabla f_T - A \nabla f_S\|_{\mathcal{D}}^2 \\ &= \mathbb{E}_{x \sim \mathcal{D}} [\|\nabla f_T(x) - A \nabla f_S(x)\|_2^2]. \end{aligned} \quad (5)$$

To continue, we split ∇f_T as two terms, i.e., one on the direction on ∇f_S and one orthogonal to ∇f_S .

Denoting $\phi(x)$ as the angle between $\nabla f_T(x)$ and $\nabla f_S(x)$ in Euclidean space, we have

$$\begin{aligned} \nabla f_T(x) &= \cos(\phi(x)) \frac{\|\nabla f_T(x)\|_2}{\|\nabla f_S(x)\|_2} \nabla f_S(x) + \nabla f_T(x) - \cos(\phi(x)) \frac{\|\nabla f_T(x)\|_2}{\|\nabla f_S(x)\|_2} \nabla f_S(x) \\ &= \cos(\phi(x)) \frac{\|\nabla f_T(x)\|_2}{\|\nabla f_S(x)\|_2} \nabla f_S(x) + \mathbf{v}(x), \end{aligned} \quad (6)$$

where we denote $\mathbf{v}(x) = \nabla f_T(x) - \cos(\phi(x)) \frac{\|\nabla f_T(x)\|_2}{\|\nabla f_S(x)\|_2} \nabla f_S(x)$ for notation convenience.

We can see that $\mathbf{v}(x)$ is orthogonal to $\nabla f_S(x)$, thus $\|\mathbf{v}(x)\|_2 = \sqrt{1 - \cos^2(\phi(x))} \|\nabla f_T(x)\|_2$. Recall that actually $\tau_1(x) = \cos^2(\phi(x))$, it can be written as $\|\mathbf{v}(x)\|_2 = \sqrt{1 - \tau_1(x)} \|\nabla f_T(x)\|_2$.

Then, plugging (6) into (5) we have

$$\begin{aligned}
(5) &= \mathbb{E}_{\mathbf{x} \sim \mathcal{D}} \left[\left\| \cos(\phi(\mathbf{x})) \frac{\|\nabla f_T(\mathbf{x})\|_2}{\|\nabla f_S(\mathbf{x})\|_2} \nabla f_S(\mathbf{x}) + \mathbf{v}(\mathbf{x}) - A \nabla f_S(\mathbf{x}) \right\|_2^2 \right] \\
&= \mathbb{E}_{\mathbf{x} \sim \mathcal{D}} \left[\left\| \left(\cos(\phi(\mathbf{x})) \frac{\|\nabla f_T(\mathbf{x})\|_2}{\|\nabla f_S(\mathbf{x})\|_2} - A \right) \nabla f_S(\mathbf{x}) + \mathbf{v}(\mathbf{x}) \right\|_2^2 \right] \\
&= \mathbb{E}_{\mathbf{x} \sim \mathcal{D}} \left[\left\| \left(\cos(\phi(\mathbf{x})) \frac{\|\nabla f_T(\mathbf{x})\|_2}{\|\nabla f_S(\mathbf{x})\|_2} - A \right) \nabla f_S(\mathbf{x}) \right\|_2^2 + \|\mathbf{v}(\mathbf{x})\|_2^2 \right] \\
&= \mathbb{E}_{\mathbf{x} \sim \mathcal{D}} \left[\left\| \left(\cos(\phi(\mathbf{x})) \frac{\|\nabla f_T(\mathbf{x})\|_2}{\|\nabla f_S(\mathbf{x})\|_2} - A \right) \nabla f_S(\mathbf{x}) \right\|_2^2 + (1 - \tau_1(\mathbf{x})) \|\nabla f_T(\mathbf{x})\|_2^2 \right] \\
&= \mathbb{E}_{\mathbf{x} \sim \mathcal{D}} \left[\left\| \left(\cos(\phi(\mathbf{x})) \frac{\|\nabla f_T(\mathbf{x})\|_2}{\|\nabla f_S(\mathbf{x})\|_2} - A \right) \nabla f_S(\mathbf{x}) \right\|_2^2 \right] + \mathbb{E}_{\mathbf{x} \sim \mathcal{D}} (1 - \tau_1(\mathbf{x})) \|\nabla f_T(\mathbf{x})\|_2^2 \\
&= \mathbb{E}_{\mathbf{x} \sim \mathcal{D}} \left[\left(\cos(\phi(\mathbf{x})) \frac{\|\nabla f_T(\mathbf{x})\|_2}{\|\nabla f_S(\mathbf{x})\|_2} - A \right)^2 \|\nabla f_S(\mathbf{x})\|_2^2 \right] + \mathbb{E}_{\mathbf{x} \sim \mathcal{D}} (1 - \tau_1(\mathbf{x})) \|\nabla f_T(\mathbf{x})\|_2^2.
\end{aligned} \tag{7}$$

Now let us deal with the first term by plugging in

$$A = \frac{\langle \Delta_{f_T, \delta_{f_S}}, \Delta_{f_S, \delta_{f_S}} \rangle_{\mathcal{D}}}{\|\Delta_{f_S, \delta_{f_S}}\|_{\mathcal{D}}^2},$$

where $\Delta_{f_T, \delta_{f_S}}(\mathbf{x}) = \epsilon \cos(\phi(\mathbf{x})) \|\nabla f_T(\mathbf{x})\|_2$ and $\Delta_{f_S, \delta_{f_S}}(\mathbf{x}) = \epsilon \|\nabla f_S(\mathbf{x})\|_2$, and we have

$$\begin{aligned}
&\mathbb{E}_{\mathbf{x} \sim \mathcal{D}} \left(\cos(\phi(\mathbf{x})) \frac{\|\nabla f_T(\mathbf{x})\|_2}{\|\nabla f_S(\mathbf{x})\|_2} - A \right)^2 \|\nabla f_S(\mathbf{x})\|_2^2 \\
&= \mathbb{E}_{\mathbf{x} \sim \mathcal{D}} (\cos(\phi(\mathbf{x})) \|\nabla f_T(\mathbf{x})\|_2 - A \|\nabla f_S(\mathbf{x})\|_2)^2 \\
&= \frac{1}{\epsilon^2} \mathbb{E}_{\mathbf{x} \sim \mathcal{D}} \left(\Delta_{f_T, \delta_{f_S}}(\mathbf{x}) - A \Delta_{f_S, \delta_{f_S}}(\mathbf{x}) \right)^2 \\
&= \frac{1}{\epsilon^2} \mathbb{E}_{\mathbf{x} \sim \mathcal{D}} \left(\Delta_{f_T, \delta_{f_S}}(\mathbf{x})^2 + A^2 \Delta_{f_S, \delta_{f_S}}(\mathbf{x})^2 - 2A \Delta_{f_T, \delta_{f_S}}(\mathbf{x}) \Delta_{f_S, \delta_{f_S}}(\mathbf{x}) \right) \\
&= \frac{1}{\epsilon^2} \left(\left\| \Delta_{f_T, \delta_{f_S}} \right\|_{\mathcal{D}}^2 + A^2 \left\| \Delta_{f_S, \delta_{f_S}} \right\|_{\mathcal{D}}^2 - 2A \langle \Delta_{f_T, \delta_{f_S}}, \Delta_{f_S, \delta_{f_S}} \rangle_{\mathcal{D}} \right) \\
&= \frac{1}{\epsilon^2} \left(\left\| \Delta_{f_T, \delta_{f_S}} \right\|_{\mathcal{D}}^2 + \frac{\langle \Delta_{f_T, \delta_{f_S}}, \Delta_{f_S, \delta_{f_S}} \rangle_{\mathcal{D}}^2}{\|\Delta_{f_S, \delta_{f_S}}\|_{\mathcal{D}}^2} - 2 \frac{\langle \Delta_{f_T, \delta_{f_S}}, \Delta_{f_S, \delta_{f_S}} \rangle_{\mathcal{D}}^2}{\|\Delta_{f_S, \delta_{f_S}}\|_{\mathcal{D}}^2} \right) \\
&= \frac{\left\| \Delta_{f_T, \delta_{f_S}} \right\|_{\mathcal{D}}^2}{\epsilon^2} \left(1 - \frac{\langle \Delta_{f_T, \delta_{f_S}}, \Delta_{f_S, \delta_{f_S}} \rangle_{\mathcal{D}}^2}{\|\Delta_{f_S, \delta_{f_S}}\|_{\mathcal{D}}^2 \cdot \|\Delta_{f_T, \delta_{f_S}}\|_{\mathcal{D}}^2} \right) \\
&= (1 - \tau_2) \mathbb{E}_{\mathbf{x} \sim \mathcal{D}} [\cos^2(\mathbf{x}) \|\nabla f_T(\mathbf{x})\|_2^2] \\
&= (1 - \tau_2) \mathbb{E}_{\mathbf{x} \sim \mathcal{D}} [\tau_1(\mathbf{x}) \|\nabla f_T(\mathbf{x})\|_2^2].
\end{aligned} \tag{8}$$

Plugging (8) into (7), we finally have

$$\begin{aligned}
&\|\nabla f_T - \nabla(g \circ f_S)\|_{\mathcal{D}}^2 \\
&= (1 - \tau_2) \mathbb{E}_{\mathbf{x} \sim \mathcal{D}} [\tau_1(\mathbf{x}) \|\nabla f_T(\mathbf{x})\|_2^2] + \mathbb{E}_{\mathbf{x} \sim \mathcal{D}} (1 - \tau_1(\mathbf{x})) \|\nabla f_T(\mathbf{x})\|_2^2 \\
&= \mathbb{E}_{\mathbf{x} \sim \mathcal{D}} [(1 - \tau_2 \tau_1(\mathbf{x})) \|\nabla f_T(\mathbf{x})\|_2^2] \\
&\leq (1 - \tau_1 \tau_2) L^2,
\end{aligned}$$

which completes the proof. \square

D Proof of Theorem 2

Theorem 2 (Restated). For two functions $f_S : \mathbb{R}^n \rightarrow \mathbb{R}^m$, and $f_T : \mathbb{R}^n \rightarrow \mathbb{R}^d$, there is an affine function $g : \mathbb{R}^m \rightarrow \mathbb{R}^d$, so that

$$\|\nabla f_T - \nabla(g \circ f_S)\|_{\mathcal{D}}^2 \leq 5\mathbb{E}_{\mathbf{x} \sim \mathcal{D}} \left(\begin{array}{l} ((1 - \tau_1(\mathbf{x})\tau_2) + (1 - \tau_1(\mathbf{x}))(1 - \tau_2)\lambda_{f_T}(\mathbf{x})^2) \|\nabla f_T(\mathbf{x})\|_2^2 \\ + (\lambda_{f_T}(\mathbf{x}) + \lambda_{f_S}(\mathbf{x}))^2 \frac{\|\nabla f_S(\mathbf{x})\|_2^2}{\|\nabla f_S\|_{\mathcal{D},2}^2} \|\nabla f_T\|_{\mathcal{D},2}^2 \end{array} \right),$$

where g is defined as $g(\mathbf{z}) = \mathbf{A}\mathbf{z} + \text{Const.}$

Moreover, if assuming that f_T is L -Lipschitz continuous, i.e., $\|\nabla f_T(\mathbf{x})\|_2 \leq L$ for $\forall \mathbf{x} \sim \text{supp}(\mathcal{D})$, and considering the worst-case singular value ratio λ , we can have a more elegant statement:

$$\|\nabla f_T - \nabla(g \circ f_S)\|_{\mathcal{D}}^2 \leq \left((1 - \tau_1\tau_2) + (1 - \tau_1)(1 - \tau_2)\lambda_{f_T}^2 + (\lambda_{f_T} + \lambda_{f_S})^2 \right) 5L^2.$$

Proof. Recall that the matrix \mathbf{A} is defined in Definition 3, i.e.,

$$\mathbf{A} = \text{proj}(\mathbb{E}_{\mathbf{x} \sim \mathcal{D}}[\Delta_{f_T, \delta_{f_S}}(\mathbf{x})\Delta_{f_S, \delta_{f_S}}(\mathbf{x})^\top] \left(\mathbb{E}_{\mathbf{x} \sim \mathcal{D}}[\Delta_{f_S, \delta_{f_S}}(\mathbf{x})\Delta_{f_S, \delta_{f_S}}(\mathbf{x})^\top] \right)^\dagger, \frac{\|\Delta_{f_T, \delta_{f_S}}\|_{\mathcal{D}}}{\|\Delta_{f_S, \delta_{f_S}}\|_{\mathcal{D}}}),$$

and we can see

$$\begin{aligned} \|\nabla f_T - \nabla(g \circ f_S)\|_{\mathcal{D},2}^2 &= \|\nabla f_T^\top - \nabla(g \circ f_S)^\top\|_{\mathcal{D},2}^2 = \|\nabla f_T^\top - \mathbf{A}\nabla f_S^\top\|_{\mathcal{D},2}^2 \\ &= \mathbb{E}_{\mathbf{x} \sim \mathcal{D}} \|\nabla f_T(\mathbf{x})^\top - \mathbf{A}\nabla f_S(\mathbf{x})^\top\|_2^2 \\ &= \mathbb{E}_{\mathbf{x} \sim \mathcal{D}} \max_{\|\mathbf{t}\|_2=1} \|\nabla f_T(\mathbf{x})^\top \mathbf{t} - \mathbf{A}\nabla f_S(\mathbf{x})^\top \mathbf{t}\|_2^2, \end{aligned} \quad (9)$$

where the last equality is due to the definition of matrix spectral norm.

Denoting ∇f^\top as either the Jacobian matrix ∇f_T^\top or ∇f_S^\top , Singular Value Decomposition (SVD) suggests that $\nabla f(\mathbf{x})^\top = \mathbf{U}\Sigma\mathbf{V}^\top$, where Σ is a diagonal matrix containing all singular values ordered by their absolute values. Let $\sigma_1, \dots, \sigma_n$ denote ordered singular values. Nothing that the number of singular values that are non-zero may be less than n , so we fill the empty with zeros, such that each of them have corresponding singular vectors, i.e., the column vectors $\mathbf{v}_1, \dots, \mathbf{v}_n$ in \mathbf{V} . That is being said, $\forall i \in [n]$, we have

$$\|\nabla f(\mathbf{x})^\top \mathbf{v}_i\|_2 = |\sigma_i|.$$

Let θ_i and \mathbf{v}_i denote the singular values and vectors for $\nabla f_S(\mathbf{x})^\top$. Noting that $\{\mathbf{v}_i\}_{i=1}^n$ define a orthonormal basis for \mathbb{R}^n , we can represent

$$\mathbf{t} = \sum_{i=1}^n \theta_i \mathbf{v}_i, \quad (10)$$

where $\sum_{i=1}^n \theta_i^2 = 1$.

As adversarial attack is about the largest eigenvalue of the gradient, plugging (10) into (9), we can split it into two parts, i.e.,

$$\begin{aligned} (9) &= \mathbb{E}_{\mathbf{x} \sim \mathcal{D}} \max_{\|\mathbf{t}\|_2=1} \left\| \nabla f_T(\mathbf{x})^\top \left(\sum_{i=1}^n \theta_i \mathbf{v}_i \right) - \mathbf{A}\nabla f_S(\mathbf{x})^\top \left(\sum_{i=1}^n \theta_i \mathbf{v}_i \right) \right\|_2^2 \\ &= \mathbb{E}_{\mathbf{x} \sim \mathcal{D}} \max_{\|\mathbf{t}\|_2=1} \left\| \begin{array}{l} \nabla f_T(\mathbf{x})^\top (\theta_1 \mathbf{v}_1) - \mathbf{A}\nabla f_S(\mathbf{x})^\top (\theta_1 \mathbf{v}_1) \\ + \nabla f_T(\mathbf{x})^\top \left(\sum_{i=2}^n \theta_i \mathbf{v}_i \right) - \mathbf{A}\nabla f_S(\mathbf{x})^\top \left(\sum_{i=2}^n \theta_i \mathbf{v}_i \right) \end{array} \right\|_2^2. \end{aligned} \quad (11)$$

Denoting $\mathbf{u} = \sum_{i=2}^n \theta_i \mathbf{v}_i$, we can see this vector is orthogonal to \mathbf{v}_1 . Let us denote \mathbf{v}'_1 as the singular vector with the biggest absolute singular value of $\nabla f_T(\mathbf{x})^\top$, parallel with attack δ_{f_T} . Now we split

$\mathbf{u} = \mathbf{u}_1 + \mathbf{u}_2$ into two terms, where \mathbf{u}_1 is parallel to \mathbf{v}'_1 , and \mathbf{u}_2 is orthogonal to \mathbf{u}_1 . As \mathbf{u}_1 is in the orthogonal space to \mathbf{v}_1 while parallel with \mathbf{v}'_1 , it is bounded by the sine value of the angle between \mathbf{v}_1 and \mathbf{v}'_1 , i.e., $\sqrt{1 - \tau_1(\mathbf{x})}$. Hence, noting that \mathbf{u} is part of the unit vector \mathbf{t} ,

$$\|\mathbf{u}_1\|_2 \leq \sqrt{1 - \tau_1(\mathbf{x})} \|\mathbf{u}\|_2 \leq \sqrt{1 - \tau_1(\mathbf{x})}. \quad (12)$$

Plugging \mathbf{u} in (11), we have

$$\begin{aligned} (11) &= \mathbb{E}_{\mathbf{x} \sim \mathcal{D}} \max_{\|\mathbf{t}\|_2=1} \left\| \begin{array}{l} \nabla f_T(\mathbf{x})^\top (\theta_1 \mathbf{v}_1) - \mathbf{A} \nabla f_S(\mathbf{x})^\top (\theta_1 \mathbf{v}_1) \\ + \nabla f_T(\mathbf{x})^\top (\mathbf{u}_1 + \mathbf{u}_2) - \mathbf{A} \nabla f_S(\mathbf{x})^\top \mathbf{u} \end{array} \right\|_2^2 \\ &\leq \mathbb{E}_{\mathbf{x} \sim \mathcal{D}} \max_{\|\mathbf{t}\|_2=1} \left(\underbrace{\|\nabla f_T(\mathbf{x})^\top (\theta_1 \mathbf{v}_1) - \mathbf{A} \nabla f_S(\mathbf{x})^\top (\theta_1 \mathbf{v}_1)\|_2}_{X_1} \right. \\ &\quad \left. + \underbrace{\|\nabla f_T(\mathbf{x})^\top \mathbf{u}_1\|_2}_{X_2} + \underbrace{\|\nabla f_T(\mathbf{x})^\top \mathbf{u}_2 - \mathbf{A} \nabla f_S(\mathbf{x})^\top \mathbf{u}\|_2}_{X_3} \right)^2, \end{aligned} \quad (13)$$

where the inequality is due to triangle inequality.

There are three terms we have to deal with, i.e., X_1 , X_2 and X_3 . Regarding the first term, \mathbf{v}_1 in X_1 aligns with the attack $\delta_{f_S}(\mathbf{x})$, which we have known through adversarial attack. The second term X_2 is trivially bounded by (12). Although adversarial attacks tell us nothing about X_3 , it can be bounded by the second largest singular values.

Let us first deal with two easiest, i.e., X_2 and X_3 . Applying (12) on X_2 directly, we have

$$X_2 = \|\nabla f_T(\mathbf{x})^\top\|_2 \cdot \|\mathbf{u}_1\|_2 \leq \sqrt{1 - \tau_1(\mathbf{x})} \|\nabla f_T(\mathbf{x})^\top\|_2.$$

For X_3 , noting that \mathbf{u}_2 is orthogonal to \mathbf{v}'_1 , and \mathbf{u} is orthogonal to \mathbf{v}_1 , we can see that \mathbf{u}_2 has no components of the largest absolute singular vector of $\nabla f_T(\mathbf{x})^\top$, and \mathbf{u} has no components of the largest absolute singular vector of $\nabla f_T(\mathbf{x})^\top$. Therefore,

$$\begin{aligned} X_3 &\leq \|\nabla f_T(\mathbf{x})^\top \mathbf{u}_2\|_2 + \|\mathbf{A} \nabla f_S(\mathbf{x})^\top \mathbf{u}\|_2 \\ &\leq \sigma_{f_T,2}(\mathbf{x}) \|\mathbf{u}_2\|_2 + \sigma_{f_S,2}(\mathbf{x}) \|\mathbf{A}\|_2 \|\mathbf{u}\|_2 \\ &= \lambda_{f_T}(\mathbf{x}) \|\nabla f_T(\mathbf{x})^\top\|_2 \|\mathbf{u}_2\|_2 + \lambda_{f_S}(\mathbf{x}) \|\nabla f_S(\mathbf{x})^\top\|_2 \|\mathbf{A}\|_2 \|\mathbf{u}\|_2 \\ &\leq \lambda_{f_T}(\mathbf{x}) \|\nabla f_T(\mathbf{x})^\top\|_2 + \lambda_{f_S}(\mathbf{x}) \|\nabla f_S(\mathbf{x})^\top\|_2 \|\mathbf{A}\|_2, \end{aligned}$$

where the first inequality is due to triangle inequality, the second inequity is done by the attributes of singular values, and the definition of matrix 2-norm. The equality is done simply by applying the definition of singular values ratio (Definition 4), and the third inequality is due to the fact that $\|\mathbf{u}_2\|_2 \leq \|\mathbf{u}\|_2 \leq 1$.

Before dealing with X_1 , let us simplify (13) by relax the square of summed terms to sum of squared terms, as the following.

$$\begin{aligned} (13) &= \mathbb{E}_{\mathbf{x} \sim \mathcal{D}} \max_{\|\mathbf{t}\|_2=1} (X_1 + X_2 + X_3)^2 \\ &= \mathbb{E}_{\mathbf{x} \sim \mathcal{D}} \max_{\|\mathbf{t}\|_2=1} X_1^2 + X_2^2 + X_3^2 + 2X_1X_2 + 2X_2X_3 + 2X_1X_3 \\ &\leq \mathbb{E}_{\mathbf{x} \sim \mathcal{D}} \max_{\|\mathbf{t}\|_2=1} X_1^2 + X_2^2 + X_3^2 + 2 \max\{X_1^2, X_2^2\} + 2 \max\{X_2^2, X_3^2\} + 2 \max\{X_1^2, X_3^2\} \\ &\leq \mathbb{E}_{\mathbf{x} \sim \mathcal{D}} \max_{\|\mathbf{t}\|_2=1} X_1^2 + X_2^2 + X_3^2 + 2(X_1^2 + X_2^2) + 2(X_2^2 + X_3^2) + 2(X_1^2 + X_3^2) \\ &= \mathbb{E}_{\mathbf{x} \sim \mathcal{D}} \max_{\|\mathbf{t}\|_2=1} 5(X_1^2 + X_2^2 + X_3^2). \end{aligned} \quad (14)$$

We note that this relaxation is not necessary, but simply for the simplicity of the final results without breaking what our theory suggests.

Bring what we have about X_2 and X_3 , and noting that $\theta_1 \leq 1$ depends on \mathbf{t} , we can drop the max operation by

$$\begin{aligned}
(14) &= \mathbb{E}_{\mathbf{x} \sim \mathcal{D}} \max_{\|\mathbf{t}\|_2=1} 5(X_1^2 + X_2^2 + X_3^2) \\
&= \mathbb{E}_{\mathbf{x} \sim \mathcal{D}} \max_{\|\mathbf{t}\|_2=1} 5(\|\nabla f_T(\mathbf{x})^\top (\theta_1 \mathbf{v}_1) - \mathbf{A} \nabla f_S(\mathbf{x})^\top (\theta_1 \mathbf{v}_1)\|_2^2 + X_2^2 + X_3^2) \\
&\leq 5 \mathbb{E}_{\mathbf{x} \sim \mathcal{D}} \left(\|\nabla f_T(\mathbf{x})^\top \mathbf{v}_1 - \mathbf{A} \nabla f_S(\mathbf{x})^\top \mathbf{v}_1\|_2^2 + (1 - \tau_1(\mathbf{x})) \|\nabla f_T(\mathbf{x})\|_2^2 \right. \\
&\quad \left. + ((\lambda_{f_T}(\mathbf{x}) + \lambda_{f_S}(\mathbf{x})) \|\nabla f_S(\mathbf{x})^\top\|_2 \|\mathbf{A}\|_2)^2 \right). \tag{15}
\end{aligned}$$

Now, let us deal with the first term. As \mathbf{v}_1 is a unit vector and is in fact the direction of $f_S(\mathbf{x})$'s adversarial attack, we can write $\delta_{f_S, \epsilon}(\mathbf{x}) = \epsilon \mathbf{v}_1$. Hence,

$$\begin{aligned}
&\mathbb{E}_{\mathbf{x} \sim \mathcal{D}} \|\nabla f_T(\mathbf{x})^\top \mathbf{v}_1 - \mathbf{A} \nabla f_S(\mathbf{x})^\top \mathbf{v}_1\|_2^2 \\
&= \mathbb{E}_{\mathbf{x} \sim \mathcal{D}} \frac{1}{\epsilon^2} \|\nabla f_T(\mathbf{x})^\top \delta_{f_S, \epsilon}(\mathbf{x}) - \mathbf{A} \nabla f_S(\mathbf{x})^\top \delta_{f_S, \epsilon}(\mathbf{x})\|_2^2 \\
&= \mathbb{E}_{\mathbf{x} \sim \mathcal{D}} \frac{1}{\epsilon^2} \left\| \Delta_{f_T, \delta_{f_S}}(\mathbf{x}) - \mathbf{A} \Delta_{f_S, \delta_{f_S}}(\mathbf{x}) \right\|_2^2, \tag{16}
\end{aligned}$$

where the last equality is derived by applying the definition of $\Delta(\mathbf{x})$, i.e., equation (1). Note that we omit the ϵ in $\delta_{f_S, \epsilon}$ for notation simplicity.

The matrix \mathbf{A} is deigned to minimize (16), as shown in the proof of Proposition 1. Expanding the term we have

$$\begin{aligned}
(16) &= \frac{1}{\epsilon^2} \mathbb{E}_{\mathbf{x} \sim \mathcal{D}} \left[\left\| \Delta_{f_T, \delta_{f_S}}(\mathbf{x}) \right\|_2^2 + \left\| \mathbf{A} \Delta_{f_S, \delta_{f_S}}(\mathbf{x}) \right\|_2^2 - 2 \langle \Delta_{f_T, \delta_{f_S}}(\mathbf{x}), \mathbf{A} \Delta_{f_S, \delta_{f_S}}(\mathbf{x}) \rangle \right] \\
&= \frac{1}{\epsilon^2} \left(\left\| \Delta_{f_T, \delta_{f_S}} \right\|_{\mathcal{D}}^2 + \left\| \mathbf{A} \Delta_{f_S, \delta_{f_S}} \right\|_{\mathcal{D}}^2 - 2 \langle \Delta_{f_T, \delta_{f_S}}, \mathbf{A} \Delta_{f_S, \delta_{f_S}} \rangle_{\mathcal{D}} \right) \\
&= \frac{\left\| \Delta_{f_T, \delta_{f_S}} \right\|_{\mathcal{D}}^2}{\epsilon^2} (1 - \tau_2) \\
&= (1 - \tau_2) \mathbb{E}_{\mathbf{x} \sim \mathcal{D}} \|\nabla f_T(\mathbf{x})^\top \mathbf{v}_1\|_2^2. \tag{17}
\end{aligned}$$

Recall that \mathbf{v}_1 is a unit vector aligns the direction of δ_{f_S} , and we have used \mathbf{v}'_1 to denote a unit vector that aligns the direction of δ_{f_T} . As τ_1 tells us about the angle between the two, let us split \mathbf{v}_1 into to orthogonal vectors, i.e., $\mathbf{v}_1 = \sqrt{\tau_1(\mathbf{x})} \mathbf{v}'_1 + \sqrt{1 - \tau_1(\mathbf{x})} \mathbf{v}'_{1, \perp}$, where $\mathbf{v}'_{1, \perp}$ is a unit vector that is orthogonal to \mathbf{v}'_1 .

Plugging this into (17) we have

$$\begin{aligned}
(17) &= (1 - \tau_2) \mathbb{E}_{\mathbf{x} \sim \mathcal{D}} \left\| \nabla f_T(\mathbf{x})^\top (\sqrt{\tau_1(\mathbf{x})} \mathbf{v}'_1 + \sqrt{1 - \tau_1(\mathbf{x})} \mathbf{v}'_{1, \perp}) \right\|_2^2 \\
&= (1 - \tau_2) \mathbb{E}_{\mathbf{x} \sim \mathcal{D}} \left[\left\| \nabla f_T(\mathbf{x})^\top \sqrt{\tau_1(\mathbf{x})} \mathbf{v}'_1 \right\|_2^2 + \left\| \nabla f_T(\mathbf{x})^\top \sqrt{1 - \tau_1(\mathbf{x})} \mathbf{v}'_{1, \perp} \right\|_2^2 \right] \\
&= (1 - \tau_2) \mathbb{E}_{\mathbf{x} \sim \mathcal{D}} \left[\tau_1(\mathbf{x}) \|\nabla f_T(\mathbf{x})^\top\|_2^2 + (1 - \tau_1(\mathbf{x})) \lambda_{f_T}(\mathbf{x})^2 \|\nabla f_T(\mathbf{x})^\top\|_2^2 \right],
\end{aligned}$$

where the second equality is due to the image of \mathbf{v}'_1 and $\mathbf{v}'_{1, \perp}$ after linear transformation $\nabla f_T(\mathbf{x})^\top$ are orthogonal, which can be easily observed through SVD.

Plugging this in (15), and with some regular algebra manipulation, finally we have

$$\begin{aligned}
(15) &= 5\mathbb{E}_{\mathbf{x} \sim \mathcal{D}} \left(\begin{array}{l} (1 - \tau_2) \left[\tau_1(\mathbf{x}) \|\nabla f_T(\mathbf{x})^\top\|_2^2 + (1 - \tau_1(\mathbf{x})) \lambda_{f_T}(\mathbf{x})^2 \|\nabla f_T(\mathbf{x})^\top\|_2^2 \right] \\ \quad + (1 - \tau_1(\mathbf{x})) \|\nabla f_T(\mathbf{x})\|_2^2 \\ \quad + (\lambda_{f_T}(\mathbf{x}) + \lambda_{f_S}(\mathbf{x}))^2 \|\nabla f_S(\mathbf{x})^\top\|_2^2 \|\mathbf{A}\|_2^2 \end{array} \right) \\
&= 5\mathbb{E}_{\mathbf{x} \sim \mathcal{D}} \left(\begin{array}{l} (1 - \tau_1(\mathbf{x})\tau_2) \|\nabla f_T(\mathbf{x})^\top\|_2^2 \\ \quad + (1 - \tau_1(\mathbf{x}))(1 - \tau_2) \lambda_{f_T}(\mathbf{x})^2 \|\nabla f_T(\mathbf{x})^\top\|_2^2 \\ \quad + (\lambda_{f_T}(\mathbf{x}) + \lambda_{f_S}(\mathbf{x}))^2 \|\nabla f_S(\mathbf{x})^\top\|_2^2 \|\mathbf{A}\|_2^2 \end{array} \right). \tag{18}
\end{aligned}$$

Recall that \mathbf{A} is from a norm-restricted matrix space, i.e., the \mathbf{A} is scaled so that its spectral norm is no greater than $\frac{\|\Delta_{f_T, \delta_{f_S}}\|_{\mathcal{D}}}{\|\Delta_{f_S, \delta_{f_S}}\|_{\mathcal{D}}}$, thus

$$\begin{aligned}
\|\mathbf{A}\|_2^2 &\leq \frac{\|\Delta_{f_T, \delta_{f_S}}\|_{\mathcal{D}}^2}{\|\Delta_{f_S, \delta_{f_S}}\|_{\mathcal{D}}^2} \leq \frac{\|\Delta_{f_T, \delta_{f_T}}\|_{\mathcal{D}}^2}{\|\Delta_{f_S, \delta_{f_S}}\|_{\mathcal{D}}^2} \\
&= \frac{\mathbb{E}_{\mathbf{x} \sim \mathcal{D}} \|\Delta_{f_T, \delta_{f_T}}(\mathbf{x})\|_2^2}{\mathbb{E}_{\mathbf{x} \sim \mathcal{D}} \|\Delta_{f_S, \delta_{f_S}}(\mathbf{x})\|_2^2} = \frac{\mathbb{E}_{\mathbf{x} \sim \mathcal{D}} \|\nabla f_T^\top(\mathbf{x})\|_2^2}{\mathbb{E}_{\mathbf{x} \sim \mathcal{D}} \|\nabla f_S^\top(\mathbf{x})\|_2^2} \\
&= \frac{\|\nabla f_T^\top\|_{\mathcal{D}, 2}^2}{\|\nabla f_S^\top\|_{\mathcal{D}, 2}^2}. \tag{19}
\end{aligned}$$

Hence, plugging the above inequality to (18), the first statement of the theorem is proven, i.e.,

$$(18) \leq 5\mathbb{E}_{\mathbf{x} \sim \mathcal{D}} \left(\begin{array}{l} (1 - \tau_1(\mathbf{x})\tau_2) \|\nabla f_T(\mathbf{x})^\top\|_2^2 \\ \quad + (1 - \tau_1(\mathbf{x}))(1 - \tau_2) \lambda_{f_T}^2 \|\nabla f_T(\mathbf{x})^\top\|_2^2 \\ \quad + (\lambda_{f_T}(\mathbf{x}) + \lambda_{f_S}(\mathbf{x}))^2 \|\nabla f_S(\mathbf{x})^\top\|_2^2 \frac{\|\nabla f_T^\top\|_{\mathcal{D}, 2}^2}{\|\nabla f_S^\top\|_{\mathcal{D}, 2}^2} \end{array} \right). \tag{20}$$

To see the second statement of the theorem, we assume f_T is L -Lipschitz continuous, i.e., $\|\nabla f_T(\mathbf{x})\|_2 \leq L$ for $\forall \mathbf{x} \in \text{supp}(\mathcal{D})$, and considering the worst-case singular value ratio $\lambda = \max_{\mathbf{x} \in \text{supp}(\mathcal{D})} \lambda_{f_S, \delta_{f_S}}$ for either f_S, f_T , we can continue as

$$\begin{aligned}
(20) &\leq 5 \left(\begin{array}{l} \mathbb{E}_{\mathbf{x} \sim \mathcal{D}} \left[(1 - \tau_1(\mathbf{x})\tau_2) \|\nabla f_T(\mathbf{x})^\top\|_2^2 \right] \\ \quad + \mathbb{E}_{\mathbf{x} \sim \mathcal{D}} \left[(1 - \tau_1(\mathbf{x}))(1 - \tau_2) \lambda_{f_T}^2 \|\nabla f_T(\mathbf{x})^\top\|_2^2 \right] \\ \quad + \mathbb{E}_{\mathbf{x} \sim \mathcal{D}} \left[(\lambda_{f_T} + \lambda_{f_S})^2 \|\nabla f_S(\mathbf{x})^\top\|_2^2 \frac{\|\nabla f_T^\top\|_{\mathcal{D}, 2}^2}{\|\nabla f_S^\top\|_{\mathcal{D}, 2}^2} \right] \end{array} \right) \\
&= 5 \left(\begin{array}{l} \mathbb{E}_{\mathbf{x} \sim \mathcal{D}} \left[(1 - \tau_1(\mathbf{x})\tau_2) \|\nabla f_T(\mathbf{x})^\top\|_2^2 \right] \\ \quad + \mathbb{E}_{\mathbf{x} \sim \mathcal{D}} \left[(1 - \tau_1(\mathbf{x}))(1 - \tau_2) \lambda_{f_T}^2 \|\nabla f_T(\mathbf{x})^\top\|_2^2 \right] \\ \quad + (\lambda_{f_T} + \lambda_{f_S})^2 \|\nabla f_T^\top\|_{\mathcal{D}, 2}^2 \end{array} \right) \\
&= 5\mathbb{E}_{\mathbf{x} \sim \mathcal{D}} \left((1 - \tau_1(\mathbf{x})\tau_2) + (1 - \tau_1(\mathbf{x}))(1 - \tau_2) \lambda_{f_T}^2 + (\lambda_{f_T} + \lambda_{f_S})^2 \right) \|\nabla f_T(\mathbf{x})^\top\|_2^2 \\
&\leq \mathbb{E}_{\mathbf{x} \sim \mathcal{D}} \left((1 - \tau_1(\mathbf{x})\tau_2) + (1 - \tau_1(\mathbf{x}))(1 - \tau_2) \lambda_{f_T}^2 + (\lambda_{f_T} + \lambda_{f_S})^2 \right) 5L^2 \\
&= \left((1 - \tau_1\tau_2) + (1 - \tau_1)(1 - \tau_2) \lambda_{f_T}^2 + (\lambda_{f_T} + \lambda_{f_S})^2 \right) 5L^2,
\end{aligned}$$

where the first inequality is due to the definition of worst-case singular value ratio, the last inequality is by Lipschitz condition, and the last equality is done by simply applying the definition of τ_1 . \square

E Proof of Theorem 3

The idea for proving Theorem 3 is straight-forward: bounded gradients difference implies bounded function difference, and then bounded function difference implies bounded loss difference.

To begin with, let us prove the following lemma.

Lemma 1. *Without loss of generality we assume $\|\mathbf{x}\|_2 \leq 1$ for $\forall \mathbf{x} \in \text{supp}(\mathcal{D})$. Consider functions $f_S : \mathbb{R}^n \rightarrow \mathbb{R}^m$, $f_T : \mathbb{R}^n \rightarrow \mathbb{R}^d$, and an affine function $g : \mathbb{R}^m \rightarrow \mathbb{R}^d$, suggested by Theorem 1 or Theorem 2, such that $g(f_S(\mathbf{0})) = f_T(\mathbf{0})$, if both f_T, f_S are β -smooth in $\{\mathbf{x} \mid \|\mathbf{x}\| \leq 1\}$, we have*

$$\|f_T - g \circ f_S\|_{\mathcal{D}} \leq \|\nabla f_T - \nabla(g \circ f_S)\|_{\mathcal{D},2} + \left(1 + \frac{\|\nabla f_T\|_{\mathcal{D},2}}{\|\nabla f_S\|_{\mathcal{D},2}}\right) \beta.$$

Proof. Let us denote $v(\mathbf{x}) = f_T(\mathbf{x}) - g \circ f_S(\mathbf{x})$, and we can show the smoothness of $v(\cdot)$.

As $g(\cdot)$ is an affine function satisfying $g(f_S(\mathbf{0})) = f_T(\mathbf{0})$, it can be denoted as $g(\mathbf{z}) = \mathbf{A}(\mathbf{z} - f_S(\mathbf{0})) + f_T(\mathbf{0})$, where \mathbf{A} is a matrix suggested by Theorem 1 or Theorem 2. Therefore, denoting $\mathbb{B}_1 = \{\mathbf{x} \mid \|\mathbf{x}\| \leq 1\}$ as a unit ball, for $\forall \mathbf{x}, \mathbf{y} \in \mathbb{B}_1$ it holds that

$$\begin{aligned} \|\nabla v(\mathbf{x}) - \nabla v(\mathbf{y})\|_2 &= \|\nabla v(\mathbf{x})^\top - \nabla v(\mathbf{y})^\top\|_2 \\ &= \|\nabla f_T(\mathbf{x})^\top - \nabla f_T(\mathbf{y})^\top - \mathbf{A}(\nabla f_S(\mathbf{x})^\top - \nabla f_S(\mathbf{y})^\top)\|_2 \\ &\leq \|\nabla f_T(\mathbf{x})^\top - \nabla f_T(\mathbf{y})^\top\|_2 + \|\mathbf{A}(\nabla f_S(\mathbf{x})^\top - \nabla f_S(\mathbf{y})^\top)\|_2 \\ &\leq \|\nabla f_T(\mathbf{x})^\top - \nabla f_T(\mathbf{y})^\top\|_2 + \|\mathbf{A}\|_2 \|\nabla f_S(\mathbf{x})^\top - \nabla f_S(\mathbf{y})^\top\|_2, \end{aligned} \quad (21)$$

where the last second inequality is due to triangle inequality, and the last inequality is by the property of spectral norm.

Applying the β -smoothness of f_S and f_T , and noting that $\|\mathbf{A}\|_2 \leq \frac{\|\nabla f_T\|_{\mathcal{D},2}}{\|\nabla f_S\|_{\mathcal{D},2}}$ as shown in (19), we can continue as

$$\begin{aligned} (21) &\leq \beta \|\mathbf{x} - \mathbf{y}\|_2 + \|\mathbf{A}\|_2 \beta \|\mathbf{x} - \mathbf{y}\|_2 \leq \beta \|\mathbf{x} - \mathbf{y}\|_2 + \frac{\|\nabla f_T\|_{\mathcal{D},2}}{\|\nabla f_S\|_{\mathcal{D},2}} \beta \|\mathbf{x} - \mathbf{y}\|_2 \\ &= \left(1 + \frac{\|\nabla f_T\|_{\mathcal{D},2}}{\|\nabla f_S\|_{\mathcal{D},2}}\right) \beta \|\mathbf{x} - \mathbf{y}\|_2, \end{aligned}$$

which suggests that $v(\cdot)$ is $\left(1 + \frac{\|\nabla f_T\|_{\mathcal{D},2}}{\|\nabla f_S\|_{\mathcal{D},2}}\right) \beta$ -smooth.

We are ready to prove the lemma now. Applying the mean value theorem, for $\forall \mathbf{x} \in \mathbb{B}_1$, we have

$$v(\mathbf{x}) - v(\mathbf{0}) = \nabla v(\xi \mathbf{x})^\top \mathbf{x},$$

where $\xi \in (0, 1)$ is a scalar number. Subtracting $\nabla v(\mathbf{x})^\top \mathbf{x}$ on both sides give

$$\begin{aligned} v(\mathbf{x}) - v(\mathbf{0}) - \nabla v(\mathbf{x})^\top \mathbf{x} &= (\nabla v(\xi \mathbf{x}) - \nabla v(\mathbf{x}))^\top \mathbf{x} \\ \|\|v(\mathbf{x}) - v(\mathbf{0}) - \nabla v(\mathbf{x})^\top \mathbf{x}\|_2 &= \|(\nabla v(\xi \mathbf{x}) - \nabla v(\mathbf{x}))^\top \mathbf{x}\|_2 \\ \|\|v(\mathbf{x}) - v(\mathbf{0}) - \nabla v(\mathbf{x})^\top \mathbf{x}\|_2 &\leq \|(\nabla v(\xi \mathbf{x}) - \nabla v(\mathbf{x}))\|_2 \|\mathbf{x}\|_2. \end{aligned}$$

Let us denote $\beta_1 = \left(1 + \frac{\|\nabla f_T\|_{\mathcal{D},2}}{\|\nabla f_S\|_{\mathcal{D},2}}\right) \beta$ for notation convenience, and apply the definition of smoothness:

$$\|v(\mathbf{x}) - v(\mathbf{0}) - \nabla v(\mathbf{x})^\top \mathbf{x}\|_2 \leq \beta_1(1 - \xi) \|\mathbf{x}\|_2^2 \leq \beta_1. \quad (22)$$

Noting that $v(\mathbf{0}) = 0$ and applying the triangle inequality, we have

$$\|v(\mathbf{x}) - v(\mathbf{0}) - \nabla v(\mathbf{x})^\top \mathbf{x}\|_2 \geq \|v(\mathbf{x})\|_2 - \|\nabla v(\mathbf{x})^\top \mathbf{x}\|_2 \geq \|v(\mathbf{x})\|_2 - \|\nabla v(\mathbf{x})\|_2$$

Plugging it into (22), we have

$$\begin{aligned} \|v(\mathbf{x})\|_2 &\leq \beta_1 + \|\nabla v(\mathbf{x})^\top\|_2 \\ \|v(\mathbf{x})\|_2^2 &\leq \beta_1^2 + \|\nabla v(\mathbf{x})^\top\|_2^2 + 2\beta_1 \|\nabla v(\mathbf{x})^\top\|_2 \\ \mathbb{E}_{\mathbf{x} \sim \mathcal{D}} \|v(\mathbf{x})\|_2^2 &\leq \beta_1^2 + \mathbb{E}_{\mathbf{x} \sim \mathcal{D}} \|\nabla v(\mathbf{x})^\top\|_2^2 + 2\beta_1 \mathbb{E}_{\mathbf{x} \sim \mathcal{D}} \|\nabla v(\mathbf{x})^\top\|_2 \\ \mathbb{E}_{\mathbf{x} \sim \mathcal{D}} \|v(\mathbf{x})\|_2^2 &\leq \beta_1^2 + \mathbb{E}_{\mathbf{x} \sim \mathcal{D}} \|\nabla v(\mathbf{x})\|_2^2 + 2\beta_1 \mathbb{E}_{\mathbf{x} \sim \mathcal{D}} \|\nabla v(\mathbf{x})\|_2 \\ \|v\|_{\mathcal{D}}^2 &\leq \beta_1^2 + \|\nabla v\|_{\mathcal{D},2}^2 + 2\beta_1 \mathbb{E}_{\mathbf{x} \sim \mathcal{D}} \|\nabla v(\mathbf{x})\|_2 \end{aligned}$$

Applying Jensen's inequality to the last term, we get

$$\begin{aligned}
\|v\|_{\mathcal{D}}^2 &\leq \beta_1^2 + \|\nabla v\|_{\mathcal{D},2}^2 + 2\beta_1 \sqrt{\mathbb{E}_{\mathbf{x} \sim \mathcal{D}} \|\nabla v(\mathbf{x})\|_2^2} \\
&= \beta_1^2 + \|\nabla v\|_{\mathcal{D},2}^2 + 2\beta_1 \sqrt{\|\nabla v\|_{\mathcal{D},2}^2} = \beta_1^2 + \|\nabla v\|_{\mathcal{D},2}^2 + 2\beta_1 \|\nabla v\|_{\mathcal{D},2} \\
&= (\|\nabla v\|_{\mathcal{D},2} + \beta_1)^2
\end{aligned}$$

Plugging $\beta_1 = \left(1 + \frac{\|\nabla f_T\|_{\mathcal{D},2}}{\|\nabla f_S\|_{\mathcal{D},2}}\right) \beta$ and $v = f_T - g \circ f_S$ into the above inequality completes the proof. \square

With the above lemma, it is easy to show the mean squared loss on the transferred model is also bounded.

Theorem 3 (Restated). *Without loss of generality we assume $\|\mathbf{x}\|_2 \leq 1$ for $\forall \mathbf{x} \in \text{supp}(\mathcal{D})$. Consider functions $f_S : \mathbb{R}^n \rightarrow \mathbb{R}^m$, $f_T : \mathbb{R}^n \rightarrow \mathbb{R}^d$, and an affine function $g : \mathbb{R}^m \rightarrow \mathbb{R}^d$, suggested by Theorem 1 or Theorem 2, such that $g(f_S(\mathbf{0})) = f_T(\mathbf{0})$. If both f_T, f_S are β -smooth, then*

$$\|g \circ f_S - y\|_{\mathcal{D}}^2 \leq \left(\|f_T - y\|_{\mathcal{D}} + \|\nabla f_T - \nabla g \circ f_S\|_{\mathcal{D},2} + \left(1 + \frac{\|\nabla f_T\|_{\mathcal{D},2}}{\|\nabla f_S\|_{\mathcal{D},2}}\right) \beta \right)^2$$

Proof. Let us denote $\beta_1 = \left(1 + \frac{\|\nabla f_T\|_{\mathcal{D},2}}{\|\nabla f_S\|_{\mathcal{D},2}}\right) \beta$, and according to Lemma 1 we can see

$$\|f_T - g \circ f_S\|_{\mathcal{D}} \leq \|\nabla f_T - \nabla(g \circ f_S)\|_{\mathcal{D},2} + \beta_1 \quad (23)$$

Applying a standard algebra manipulation to the left hand side, and then applying triangle inequality, we have

$$\|f_T - g \circ f_S\|_{\mathcal{D}} = \|f_T - y + y - g \circ f_S\|_{\mathcal{D}} \geq \|y - g \circ f_S\|_{\mathcal{D}} - \|f_T - y\|_{\mathcal{D}}.$$

Plugging this directly into (23), it holds that

$$\begin{aligned}
\|y - g \circ f_S\|_{\mathcal{D}} - \|f_T - y\|_{\mathcal{D}} &\leq \|\nabla f_T - \nabla(g \circ f_S)\|_{\mathcal{D},2} + \beta_1 \\
\|y - g \circ f_S\|_{\mathcal{D}} &\leq \|f_T - y\|_{\mathcal{D}} + \|\nabla f_T - \nabla(g \circ f_S)\|_{\mathcal{D},2} + \beta_1
\end{aligned}$$

Replacing β_1 by $\left(1 + \frac{\|\nabla f_T\|_{\mathcal{D},2}}{\|\nabla f_S\|_{\mathcal{D},2}}\right) \beta$ and taking the square, we can see Theorem 3 is proven. \square

F Proof of Proposition 2

Proposition 2 (Restated). *If \mathcal{L}_T is mean squared loss, f_T achieves zero loss, and the attack recovers the virtual adversarial attack within an ϵ -ball (Definition 1), the empirical adversarial transferability defined in (2) is approximately upper and lower bounded by*

$$\begin{aligned}
\mathcal{L}_T(f_T \circ PGD_{f_S}; y, \mathcal{D}) &\geq \epsilon^2 \mathbb{E}_{\mathbf{x} \sim \mathcal{D}} \left[\tau_1(\mathbf{x}) \|\nabla f_T(\mathbf{x})\|_2^2 \right] + O(\epsilon^3), \\
\mathcal{L}_T(f_T \circ PGD_{f_S}; y, \mathcal{D}) &\leq \epsilon^2 \mathbb{E}_{\mathbf{x} \sim \mathcal{D}} \left[(\lambda_{f_T}^2 + (1 - \lambda_{f_T}^2) \tau_1(\mathbf{x})) \|\nabla f_T(\mathbf{x})\|_2^2 \right] + O(\epsilon^3),
\end{aligned}$$

where $O(\epsilon^3)$ denotes a cubic error term. We can see that as $\tau_1(\mathbf{x})$ becomes larger, both the lower and upper bound become larger.

Proof. Recall that the empirical adversarial transferability is defined as a loss

$$\mathcal{L}_T(f_T \circ PGD_{f_S}; y, \mathcal{D}) = \mathbb{E}_{\mathbf{x} \sim \mathcal{D}} \ell_T(f_T(PGD_{f_S}(\mathbf{x})), y(\mathbf{x})).$$

As \mathcal{L}_T is mean squared loss, and f_T achieves zero loss, i.e., $f_T = y$, we have

$$\begin{aligned}
L_{ST}(f_T \circ PGD_{f_S}; y, \mathcal{D}) &= \mathbb{E}_{\mathbf{x} \sim \mathcal{D}} \|f_T(PGD_{f_S}(\mathbf{x})) - y(\mathbf{x})\|_2^2 \\
&= \mathbb{E}_{\mathbf{x} \sim \mathcal{D}} \|f_T(PGD_{f_S}(\mathbf{x})) - f_T(\mathbf{x})\|_2^2. \quad (24)
\end{aligned}$$

If PGD_{f_S} recovers the virtual adversarial attack within an ϵ -ball, it means that

$$PGD_{f_S}(\mathbf{x}) = \mathbf{x} + \boldsymbol{\delta}_{f_S, \epsilon}(\mathbf{x}).$$

Plugging this in and it becomes

$$(24) = \mathbb{E}_{\mathbf{x} \sim \mathcal{D}} \|f_T(\mathbf{x} + \boldsymbol{\delta}_{f_S, \epsilon}(\mathbf{x})) - f_T(\mathbf{x})\|_2^2.$$

Denoting $\boldsymbol{\delta}_{f_S, \epsilon}(\mathbf{x}) = \epsilon \boldsymbol{\delta}_{f_S, 1}(\mathbf{x})$, and define an auxiliary function h as

$$h(t) = f_T(\mathbf{x} + t \boldsymbol{\delta}_{f_S, 1}(\mathbf{x})) - f_T(\mathbf{x}),$$

we can see that $\|f_T(\mathbf{x} + \boldsymbol{\delta}_{f_S, \epsilon}(\mathbf{x})) - f_T(\mathbf{x})\|_2^2 = \|h(\epsilon)\|_2^2$.

We can then apply Taylor expansion to approximate $h(\epsilon)$ with a second order error term $O(\epsilon^2)$, i.e.,

$$h(\epsilon) = \frac{\partial h}{\partial t} \Big|_{t=0} + O(\epsilon^2) = \epsilon \nabla f_T(\mathbf{x})^\top \boldsymbol{\delta}_{f_S, 1}(\mathbf{x}) + O(\epsilon^2).$$

Therefore, assuming that $\|\nabla f_T(\mathbf{x})\|_2$ is bounded for $\mathbf{x} \in \text{supp}(\mathcal{D})$, we have

$$\|f_T(\mathbf{x} + \boldsymbol{\delta}_{f_S, \epsilon}(\mathbf{x})) - f_T(\mathbf{x})\|_2^2 = \|h(\epsilon)\|_2^2 = \epsilon^2 \|\nabla f_T(\mathbf{x})^\top \boldsymbol{\delta}_{f_S, 1}(\mathbf{x})\|_2^2 + O(\epsilon^3), \quad (25)$$

where we have omit higher order error term, i.e., $O(\epsilon^4)$.

Next, let us deal with the term $\|\nabla f_T(\mathbf{x})^\top \boldsymbol{\delta}_{f_S, 1}(\mathbf{x})\|_2^2$. Same us the technique we use in the proof of Theorem 2, we split $\boldsymbol{\delta}_{f_S, 1}(\mathbf{x}) = \mathbf{v}_1 + \mathbf{v}_2$, where \mathbf{v}_1 aligns the direction of $\boldsymbol{\delta}_{f_T, 1}(\mathbf{x})$, and \mathbf{v}_2 is orthogonal to \mathbf{v}_1 . Noting that $\tau_1(\mathbf{x})$ is the squared cosine of the angle between $\boldsymbol{\delta}_{f_S, 1}(\mathbf{x})$ and $\boldsymbol{\delta}_{f_T, 1}(\mathbf{x})$, we can see that

$$\begin{aligned} \|\mathbf{v}_1\|_2^2 &= \tau_1(\mathbf{x}) \|\boldsymbol{\delta}_{f_S, 1}(\mathbf{x})\|_2^2 = \tau_1(\mathbf{x}), \\ \|\mathbf{v}_2\|_2^2 &= (1 - \tau_1(\mathbf{x})) \|\boldsymbol{\delta}_{f_S, 1}(\mathbf{x})\|_2^2 = (1 - \tau_1(\mathbf{x})). \end{aligned}$$

Therefore, we can continue as

$$\begin{aligned} \|\nabla f_T(\mathbf{x})^\top \boldsymbol{\delta}_{f_S, 1}(\mathbf{x})\|_2^2 &= \|\nabla f_T(\mathbf{x})^\top (\mathbf{v}_1 + \mathbf{v}_2)\|_2^2 \\ &= \|\nabla f_T(\mathbf{x})^\top \mathbf{v}_1\|_2^2 + \|\nabla f_T(\mathbf{x})^\top \mathbf{v}_2\|_2^2 \\ &= \tau_1(\mathbf{x}) \|\nabla f_T(\mathbf{x})\|_2^2 + \|\nabla f_T(\mathbf{x})^\top \mathbf{v}_2\|_2^2, \end{aligned} \quad (26)$$

where the second equality is because that \mathbf{v}_1 is corresponding to the largest singular value of $\nabla f_T(\mathbf{x})^\top$, and \mathbf{v}_2 is orthogonal to \mathbf{v}_1 .

Next, we derive the lower bound and upper bound for (26). The lower bounded can be derived as

$$\tau_1(\mathbf{x}) \|\nabla f_T(\mathbf{x})\|_2^2 + \|\nabla f_T(\mathbf{x})^\top \mathbf{v}_2\|_2^2 \geq \tau_1(\mathbf{x}) \|\nabla f_T(\mathbf{x})\|_2^2,$$

and the upper bounded can be derived as

$$\begin{aligned} \tau_1(\mathbf{x}) \|\nabla f_T(\mathbf{x})\|_2^2 + \|\nabla f_T(\mathbf{x})^\top \mathbf{v}_2\|_2^2 &\leq \tau_1(\mathbf{x}) \|\nabla f_T(\mathbf{x})\|_2^2 + \lambda_{f_T}(\mathbf{x})^2 \|\nabla f_T(\mathbf{x})\|_2^2 \|\mathbf{v}_2\|_2^2 \\ &= \tau_1(\mathbf{x}) \|\nabla f_T(\mathbf{x})\|_2^2 + \lambda_{f_T}(\mathbf{x})^2 \|\nabla f_T(\mathbf{x})\|_2^2 (1 - \tau_1(\mathbf{x})) \\ &\leq \tau_1(\mathbf{x}) \|\nabla f_T(\mathbf{x})\|_2^2 + \lambda_{f_T}^2 \|\nabla f_T(\mathbf{x})\|_2^2 (1 - \tau_1(\mathbf{x})) \\ &= (\lambda_{f_T}^2 + (1 - \lambda_{f_T}^2) \tau_1(\mathbf{x})) \|\nabla f_T(\mathbf{x})\|_2^2, \end{aligned}$$

where $\lambda_{f_T}(\mathbf{x})$ is the singular value ratio of f_T at \mathbf{x} , and λ_{f_T} is the maximal singular value of f_T .

Applying the lower and upper bound to (25), we finally have

$$\begin{aligned} \|f_T(\mathbf{x} + \boldsymbol{\delta}_{f_S, \epsilon}(\mathbf{x})) - f_T(\mathbf{x})\|_2^2 &\geq \epsilon^2 \tau_1(\mathbf{x}) \|\nabla f_T(\mathbf{x})\|_2^2 + O(\epsilon^3), \\ \|f_T(\mathbf{x} + \boldsymbol{\delta}_{f_S, \epsilon}(\mathbf{x})) - f_T(\mathbf{x})\|_2^2 &\leq \epsilon^2 (\lambda_{f_T}^2 + (1 - \lambda_{f_T}^2) \tau_1(\mathbf{x})) \|\nabla f_T(\mathbf{x})\|_2^2 + O(\epsilon^3). \end{aligned} \quad (27)$$

Noting that

$$L_{ST}(f_T \circ PGD_{f_S}; y, \mathcal{D}) = \mathbb{E}_{\mathbf{x} \sim \mathcal{D}} \|f_T(\mathbf{x} + \boldsymbol{\delta}_{f_S, \epsilon}(\mathbf{x})) - f_T(\mathbf{x})\|_2^2,$$

we can see that taking expectation to (27) completes the proof. \square

G Experiment Details

All experiments are conducted on 4 RTX 2080 Ti GPUs and in python3 Ubuntu 16.04 environment.

G.1 Adversarial Transferability Indicates Knowledge-transfer among Data Distributions

Details of Model Training To provide a fair comparison, we train five source models on the five source datasets from 0% animals to 100% animals, and one reference models on STL-10 with identical architectures and hyperparameters. We use SGD optimizer and standard cross-entropy loss with learning rate 0.1, momentum 0.9, and weight decay 10^{-4} . Each model is trained for 300 epochs.

G.2 Adversarial Transferability Indicating Knowledge-transfer among Attributes

Details of Model Training We train 40 binary source classifiers on each of the 40 attributes of CelebA with ResNet18 [21]. All the classifiers are trained with optimizer Adadelta with a learning rate of 1.0 for 14 epochs. We also train a facial recognition model as a reference model on CelebA with 10,177 identities using ResNet18 as the controlled experiment. The reference facial recognition model is optimized with SGD and initial learning rate 0.1 on the ArcFace [9] with focal loss [37] for 125 epochs. For each source model, we construct a transferred model by stripping off the last layers and attaching a facial recognition head without parameters. Then we use the 40 transferred models to evaluate the knowledge transferability on 7 facial recognition benchmarks.

G.3 Adversarial Transferability Indicating Knowledge-transfer among Tasks

Details of Model Training We use 15 pretrained models released in the task bank [82] as the source models. Each source model consists of two parts, an encoder, and a decoder. The encoder is a modified ResNet50 without pooling, homogeneous across all tasks, whereas the decoder is customized to suit the output of each task. When measuring the adversarial transferability, we will use each source model as a reference model and compute the transferability matrix as described below.

Adversarial Transferability Matrix (ATM) is used here to measure the adversarial transferability between multiple tasks. In the experiment of determining similarity among tasks, it is hard to compare directly and fairly, since each task is of different loss functions, which is usually in a very different scale with each other. To solve this problem, we take the same ordinal normalization approach as [82]. Suppose we have N tasks in the pool, a tournament matrix M_T for each task T is constructed, where the element of the matrix $m_{i,j}$ represents what percentages of adversarial examples generated from the i th task transfers better to task T than the ones of the j th task (untargeted attack success rate is used here). Then we take the principal eigenvectors of the N tournament matrices and stack them together to build the $N \times N$ adversarial transferability matrix.

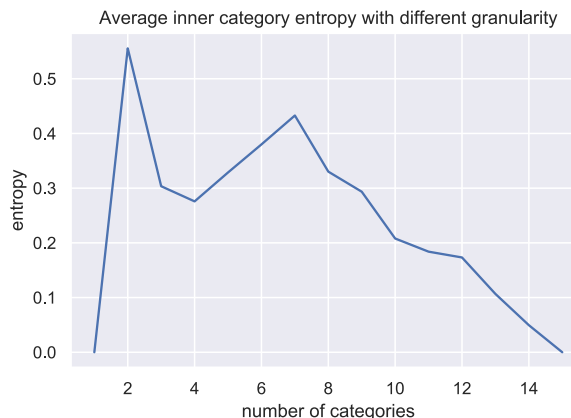


Figure 6: We also quantitatively compare our prediction with the Taskonomy [82] prediction when different number of categories is enforced. We find our prediction is similar with theirs with $n \geq 3$.